Addendum

to the
Letter of Intent

KATRIN: A next generation tritium beta decay experiment with sub-eV sensitivity for the electron neutrino mass

T. Thümmler[a,h], C. Weinheimer[a], A. Osipowicz[b], H. Blümer[c,g], G. Drexlin[c], K. Eitel[c], R. Gumbsheimer[c], H. Hucker[c], G. Meisel[c], P. Plischke[c], F. Schwamm[c], M. Steidl[c], A. Beglarian[d], H. Gemmeke[d], S. Wüstling[d], C. Day[e], R. Gehring[e], V. Hauer[e], K.-P. Jüngst[e], P. Komarek[e], W. Lehmann[e], A. Mack[e], H. Neumann[e], M. Noe[e], B. Bornschein[f], L. Dörr[f], M. Glugla[f], T. Kepcija[g], J. Reichenbacher[g], J. Wolf[g], J. Bonn[h], L. Bornschein[h], B. Flatt[h], F. Glück[h], C. Kraus[h], B. Müller[h], E.W. Otten[h], J.-P. Schall[h], V. Aseev[i], A. Belesev[i], A. Berlev[i], E. Geraskin[i], A. Golubev[i], O. Kazachenko[i], V. Lobashev[i], N. Titov[i], V. Usanov[i], S. Zadoroghny[i], O. Dragoun[j], J. Kašpar[j], A. Kovalík[j], M. Ryšavý[j], A. Špalek[j], D. Venos[j], P.J. Doe[k], S.R. Elliott[k], R.G.H. Robertson[k], J.F. Wilkerson[k]

[a] *Rheinische Friedrich-Wilhelms-Universität Bonn, Institut für Strahlen- und Kernphysik, Nussallee 14-16, 53115 Bonn, Germany*

[b] *University of Applied Sciences (FH) Fulda, Marquardtstr. 35, 36039 Fulda, Germany*

[c] *Forschungszentrum Karlsruhe, Institut für Kernphysik, Postfach 3640, 76021 Karlsruhe, Germany*

[d] *Forschungszentrum Karlsruhe, Institut für Prozessdatenverarbeitung und Elektronik, Postfach 3640, 76021 Karlsruhe, Germany*

[e] *Forschungszentrum Karlsruhe, Institut für Technische Physik, Postfach 3640, 76021 Karlsruhe, Germany*

[f] *Forschungszentrum Karlsruhe, Tritium-Labor Karlsruhe, Postfach 3640, 76021 Karlsruhe, Germany*

[g] *Universität Karlsruhe (TH), Institut für Experimentelle Kernphysik, Gaedestr. 1, 76128 Karlsruhe, Germany*

[h] *Johannes Gutenberg-Universität Mainz, Institut für Physik, 55099 Mainz, Germany*

[i] *Academy of Sciences of Russia, Institute for Nuclear Research, 60th October Anniversary Prospect 7a, 117312 Moscow, Russia*

[j] *Academy of Sciences of the Czech Republic, Nuclear Physics Institute, CZ-250 68 Řež near Prague, Czech Republic*

[k] *Center for Experimental Nuclear Physics and Astrophysics, and Department of Physics, University of Washington, Seattle, WA 98195, USA*

ABSTRACT

This Addendum to the *Letter of Intent* of the Karlsruhe Tritium Neutrino (KATRIN) experiment gives an overview of the current status of the project. KATRIN is a proposed next-generation tritium β-decay experiment, which is designed to measure the mass of the electron neutrino with a sub-eV sensitivity.
In the first part of this Addendum we report on recent developments and results in neutrino and astroparticle physics, focusing on areas which are of particular interest for the project. The second part gives an update of the design work on the key components of KATRIN and outlines the R & D progress that has been achieved over the past 8 months.

Contents

1 New Developments in Neutrino Physics

The investigation of the masses and mixings of neutrinos continues to be one of the most fundamental tasks in particle physics today with crucial implications for astrophysics and cosmology. Since the publication of the KATRIN Letter of Intent [1)] important new experimental results in neutrino physics have been obtained and theoretical models for solving neutrino-related problems in astroparticle physics have been proposed. In the following we will report on recent developments in these fields of work, outline new motivations for the KATRIN project and discuss the impact of the KATRIN measurements for various fields of cosmology and astroparticle physics.

For an introductory discussion of the rôle of neutrinos in particle physics, astrophysics and cosmology we refer to our Letter of Intent [1)] (and to references therein) as well as to more comprehensive recent review articles [2,3,4)].

1.1 Cosmology

Relic neutrinos with masses in the few-eV or sub-eV range play an active rôle as neutrino Hot Dark Matter (νHDM) in the evolution of large scale structures (LSS) in the universe [4)] due to the erasure of small-scale structures from the free-streaming of neutrinos over large distances.

The evolution of LSS can be traced by different methods. Measurements of the fluctuations of the cosmic microwave background (CMB) radiation provide an early picture of LSS formation shortly after the Big Bang [5)]. For later times up to the present epoch, the LSS distribution can be investigated by the observation of the Lyman α forest [6)], galaxy cluster abundances [7)] and, more recently, by high statistics galaxy redshift surveys [9)]. These methods should provide a self-consistent picture of the evolution of LSS, allowing to construct a cosmic 'concordance' model [10)] for the matter-energy budget of the universe. This concordance model based on CMB and LSS data currently favours a flat universe Ω_{tot}=1 with a dominant vacuum energy contribution $\Omega_\Lambda \simeq 0.7$ and a matter contribution $\Omega_m \simeq 0.3$. The latter is dominated by the Cold Dark Matter (CDM) component Ω_{CDM}, with additional contributions Ω_b from baryons and Ω_{HDM} from neutrino Hot Dark Matter.

Over the last years several limits on the sum of neutrino masses $m_{\nu,tot}$ have been reported from CMB and LSS investigations [12]. Most cosmological bounds on $m_{\nu,tot}$ give an upper limit in the range of $3-6$ eV and are thus comparable to the laboratory limit from tritium β-decay. The most recent reliable limit has been obtained in [5], yielding $m_{\nu,tot} < 4.2$ eV from a combined analysis of CMB and LSS data. In the nearer future new limits on $m_{\nu,tot}$ can be expected from the high statistics galaxy redshift surveys SDSS [8] and 2dF [9]. There are, however, potential systematic effects associated with cosmological studies. Therefore we report and comment on a recent ν-mass limit obtained from the 2dF survey, the largest effort in this field so far.

1.1.1 Galaxy Surveys

The 2dF Galaxy Redshift Survey is a survey of 220 000 galaxies with mean redshift z=0.11, which has recently announced new limits on the ν-mass[9]. To deduce a ν-mass limit, the measured distribution of galaxies has to be modelled by a matter spectrum. This requires that possible redshift-space distortions as well as biasing effects are carefully avoided. The deduced matter distribution is then fitted with a four-component matter model with Ω_Λ, Ω_{CDM}, Ω_b and the νHDM component Ω_{HDM}. It is important to note that there are degeneracies between these parameters. Thus one has to rely on further assumptions (flat universe with Ω_{tot}=1) as well as on input from other experiments for Ω_Λ, Ω_m and Ω_b and the Hubble expansion rate h. The errors associated with these input parameters imply that the ν-mass results crucially depend on the *priors* for these parameters.

The most serious degeneracies occur between Ω_m and Ω_{HDM} as well as between Ω_{HDM} and the scalar spectral index n of the matter power spectrum. Different priors for Ω_m and n result in limits for the sum of neutrino masses $m_{\nu,tot}$ which differ by factors of up to 2. A conservative set of input parameters is to use a flat prior for Ω_m from 0.1-0.5 and a spectral index of $n = 1.1$. For this parameter combination one obtains a limit of $m_{\nu,tot} < 2.2$ eV (95 % CL.) for a 3-ν quasi-degenerate mass model (the results do not change significantly if a 2-ν mass model is used instead). This would correspond to an upper limit for the electron neutrino mass m(ν_e) < 0.7 eV (95 % CL.).

In the nearer future, data from surveys with improved statistical precision will become available. However, the generic problems associated with the interpretation of LSS and CMB data will likely remain, in particular with regard to constructing matter distributions and the degeneracies of parameters in multi-dimensional fitting procedures. For these reasons, the ultimate sensitivity limit for $m_{\nu,tot}$ which can be reliably extracted by these methods is estimated to be about 1-2 eV [11].

1.1.2 KATRIN impact on cosmology

In contrast to the cosmological methods described above, the KATRIN experiment will yield a *direct* measurement of the electron neutrino mass $m(\nu_e)$. As outlined earlier [1], this value can then be used as a precise input parameter for the interpretation of the CMB and LSS data. Most importantly, a new input for Ω_{HDM} would further break the degeneracies of the different matter-energy components of the observed CMB and LSS data, thereby adding to the overall precision in the field of cosmology.

When discussing the cosmological relevance of the future KATRIN measurements, it is worth mentioning two recent results. First, there is strong experimental evidence [24,25] from the SNO experiment for the oscillations of solar ν_e to the *active* ν-flavours $\nu_{\mu,\tau}$ (this is discussed in more detail below). SNO and other solar neutrino data now point to the Large Mixing Angle (LMA) solution, which implies strong mixing among ν_e and ν_μ. If further combined with the atmospheric ν-results of the Super-Kamiokande experiment, which are explained by maximum mixing of ν_μ and ν_τ, the SNO results imply a strong (maximum or nearly maximum) mixing among ν_e, ν_μ and ν_τ. As the corresponding mass splittings are $\Delta m^2 \leq 10^{-2}$ eV^2, the ν_e-mass measurement from KATRIN will allow to determine the fundamental mass scale of neutrinos. The SNO results have thus added to the cosmological relevance of future tritium β-decay measurements.

A second cosmological implication of the LMA mixing solution is with regard to the number density of relic neutrinos. The exact number density of relic neutrinos from the standard hot Big Bang model depends on the unknown chemical potentials for the three ν-species. Usually, it is assumed that there is a negligible asymmetry between neutrinos and anti-neutrinos of the order of the baryon asymmetry of a few $\times 10^{-10}$. However, there are several cosmological models which predict rather large neutrino asymmetries. According to these models, the relic neutrino number density would not be well defined.

In a recent paper [13] this open issue has been addressed. Taking into account the effects of ν-flavour oscillations shortly after the Big Bang before the nucleosynthesis epoch, the authors conclude that effective flavour equilibrium between all active neutrino species is established, if the ν-oscillation parameters are in the range indicated by the atmospheric ν-results and the LMA solution of solar ν's. This strongly constrains possible neutrino chemical potentials, so that the number density of relic neutrinos is now known to about 1 % [13]. Consequently, existing ν-mass limits from ^{3}H β-decay as well as future measurements of $m(\nu_e)$ with KATRIN will provide unambiguous information on the neutrino mass density, essentially free of the uncertainty of neutrino chemical potentials.

1.2 Astrophysics

There are two recent developments in astrophysics which are relevant for direct ν-mass measurements. First, there are new approaches for ν-mass measurements with supernova neutrino Time-of-Flight (ToF) studies. Second, a new model has been proposed which aims at explaining the origin of ultra high energy (UHE) cosmic rays. This so-called Z-burst model would require relic neutrino masses within the m(ν_e) sensitivity range of KATRIN.

1.2.1 Supernova neutrino ToF studies

The narrow time signal of a supernova (SN) neutrino burst of less than 10 s in combination with the very long-baseline between source and detector of several kpc allows to investigate small ToF effects resulting from non-zero ν-masses [14]. Supernova ToF studies are based on the observation of the energy-dependent time delay of massive neutrinos relative to massless neutrinos. This method provides an experimental sensitivity for the rest masses of ν_e , ν_μ and ν_τ of a few tens of eV. This sensitivity can be pushed into the few-eV range, if additional assumptions on the time evolution of the ν-burst are being made. In this case the ν-mass sensitivity becomes model-dependent, however.

Recently, new methods have been proposed which do not rely on details of the ν-burst timing and which allow to achieve a sensitivity in the few-eV range for ν_μ and ν_τ also. The two most promising techniques are: a) the measurement of the abrupt termination of the SN-ν signal due to the early formation of a black hole [15,16] and b) the correlation of SN ν-signals with independent signals from gravitational wave experiments [17].

The first method relies on a scenario where the gravitational core collapse of a very massive star does not stop at the hot protoneutron star stage but proceeds further, resulting in the formation of a black hole. For short time scales of black hole formation of the order of a few seconds, the SN ν-pulse is sharply terminated, when the event horizon crosses the ν-emission sphere. This cutoff of $\mathcal{O}$ (0.5 s) can be used as a rather sharp 'time reference' to search for ν-mass effects. Detailed model calculations of this scenario have been performed in [15] for ν-masses in the few-eV range. Fig. 1 shows that the mass sensitivity of this method improves if the distance source-detector decreases. If compared to the sensitivity of present and future tritium experiments, only a nearby supernova would allow to deduce a competitive ν-mass limit. However, core collapse supernovae at distances < 1 kpc are exceedingly rare.

Instead, should future measurements reveal a SN ν-pulse, which is terminated abruptly after a few seconds, the information on the ν-mass provided by KATRIN could be used as a reliable input in the interpretation of the time structure of the ν-pulse.

A second method with the potential to yield improved ν-mass sensitivities with SN neutrinos is the time correlation of the ν-pulse with data from gravitational wave experiments. This technique has been investigated in detail in [15]. The matching of the signals from the neutronization electron neutrino flash, which could be observed by existing underground detectors like Super-Kamiokande or SNO, with the gravitational waves recorded by the gravity wave antennae soon to be operational

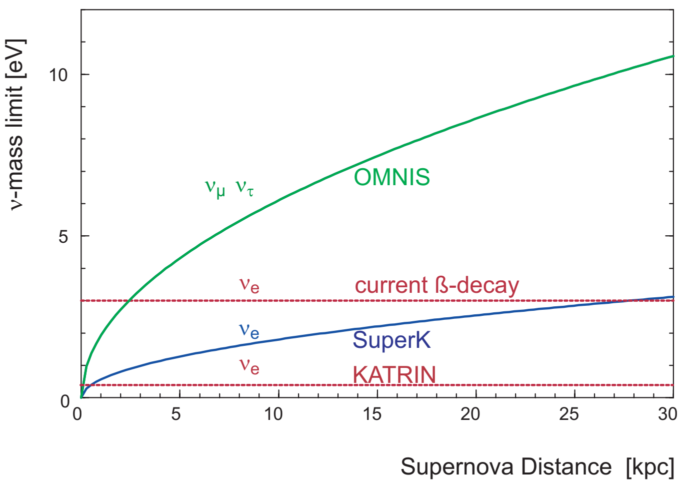

Figure 1: Comparison of the ν-mass sensitivities of astrophysical and laboratory experiments. For the model of a core collapse with early black hole formation the mass sensitivity of Super-Kamiokande for ν_e and of the proposed OMNIS experiment for ν_μ and ν_τ are shown as a function of SN distance (from [15,16]) and are compared to the ν_e mass sensitivity of present and future ^{3}H β-decay experiments.

(GEO600, LIGO, Virgo), would allow to be sensitive to an electron neutrino mass of 0.75 eV (95 % CL.), if no significant mass effect will be found. However, the results will depend to some extend on the ν_e survival probability and the details of ν-flavour oscillations or transformations occurring in the environment of the hot protoneutron star. In the case where all ν_e from the neutronization burst would be converted to ν_μ and ν_τ the sensitivity limit would be 1.1 eV (95 % CL.). Given these sensitivity estimates, the sensitivity limit of KATRIN for the electron neutrino mass would still be more stringent than these interesting and fascinating possibilities. Again, taking the argument vice versa, the neutrino mass measurement from KATRIN could contribute to a better understanding of a future SN signal, in particular with regard to the subtle effects associated with the core neutronization and the emission of gravitational waves, thus adding to a better understanding of these processes as well.

1.2.2 Ultra High Energy Cosmic Rays

A possible new interrelation between neutrino and cosmic ray physics has received a lot of interest recently [18,19,20,21]. In this so-called *Z-burst* scenario, the observed flux of ultra high energy (UHE) cosmic rays $\geq 10^{20}$ eV is explained by the resonant annihilation of UHE neutrinos with *massive* relic neutrinos into Z-bosons.

The origin and nature of the observed UHE cosmic ray events above the so-called Greisen-Zatsepin-Kuzmin (GZK) cutoff is one of the most important questions in cosmic ray physics today. Conventional scenarios for UHE cosmic rays assume that they are protons from plausible UHE sources (such as quasars) at cosmological distances. However, the GZK cutoff limits the maximum energy for UHE cosmic ray

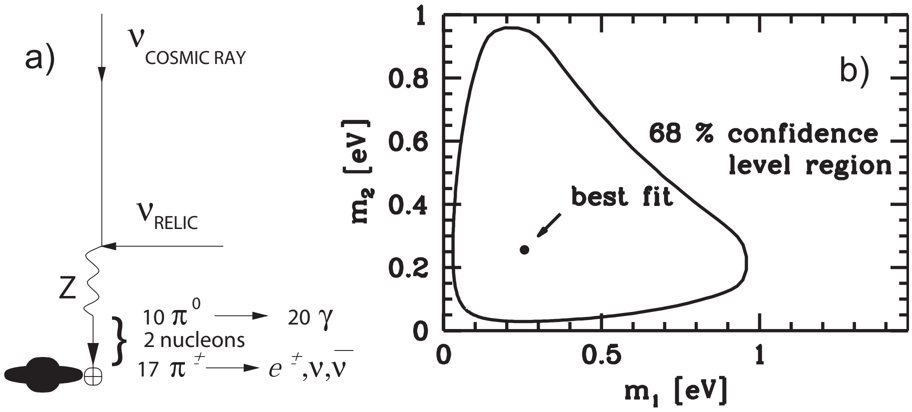

Figure 2: The Z-burst scenario for UHE cosmic rays: a) the resonant annihilation of an UHE-ν with a massive relic ν gives rise to UHE cosmic ray protons from the hadronic decay modes of the Z-boson at local distances of a few Mpc, b) neutrino mass parameters from a fit to a global data set for UHE cosmic ray energies [20].

protons from distances ≥ 50 Mpc to 4×10^{19} eV. The Z-burst scenario would evade the GZK cutoff, as UHE neutrinos with energies far above the GZK cutoff could travel over cosmological distances of several hundred Mpc without being attenuated (see fig. 2 a).

The Z-burst model requires the annihilation between the UHE-ν's and relic neutrinos to be on the Z-mass shell M_Z, so that the resonance energy $\mathrm{E}_{\nu_i}^{\mathrm{res}}$ is given by

$$E_{\nu_i}^{\mathrm{res}} = \frac{M_Z^2}{2\, m_{\nu_i}} = 4.2 \cdot 10^{21}\ \mathrm{eV} \left(\frac{1\ \mathrm{eV}}{m_{\nu_i}} \right) , \tag{1}$$

For relic neutrino masses m_{ν_i} of $\mathcal{O}\,(1\,\mathrm{eV})$, $\mathrm{E}_{\nu_i}^{\mathrm{res}}$ would be close to the highest energy cosmic rays. Several detailed calculations in the framework of this model have been performed [20,21], taking into account known parameters like Z-production and -decay as well as propagation effects, while at the same time relying on assumptions for the unknown UHE-ν fluxes and the relic neutrino number density. Quantitatively, a small relic ν-mass m_{ν_i} requires a large $\mathrm{E}_{\nu_i}^{\mathrm{res}}$ to produce a Z-boson. This relationship implies that a measurement of the shape of the UHE cosmic ray energy spectrum above a few $\times$ 10^{19} eV would allow to determine m_{ν_i}.

Fits to the available UHE cosmic ray data suffer from the rather limited statistics of the current data from AGASA, Fly's Eye and other experiments. Moreover, systematic errors in the fit procedures arise, as one has to take into account possible other contributions to the UHE cosmic ray spectrum. Both factors limit the precision of the ν-mass estimates in the Z-burst model. Most fits using reasonable input parameters yield however relic ν-masses of the order of $\mathcal{O}\,(1\ \mathrm{eV})$ eV. In [19] the mass of the heaviest relic neutrino turns out to lie in the range from 2.1 - 6.7 eV at the $1\,\sigma$ level, if there is a local background of UHE protons from the galactic neighbourhood. If this background is of extragalactic origin, neutrino masses are found to lie in the range from 0.08 - 1.3 eV (at the 68 % CL.). Finally, with no background from other sources, neutrino masses would be in the range 0.24 - 2.6 eV. This spread clearly underlines the strong model-dependence of neutrino mass estimates within the Z-burst model. In an earlier publication the same authors used a specific $2\,\nu$ degenerate mass model [20)] and obtained neutrino masses in a preferred parameter range shown in fig. 2.

There are several ways to test the Z-burst model. In the nearer future the Pierre Auger Observatory [22)] will be able to detect or set limits to the flux of UHE-neutrinos, thus constraining one of the input parameters of the Z-burst model. Auger will also measure the shape of the UHE cosmic ray energy spectrum with much better statistics, which should allow to perform an improved quantitative analysis of ν-masses in the framework of the Z-burst model. These improved ν-mass estimates could then be compared with future laboratory results from the direct measurement of the electron neutrino mass $\mathrm{m}(\nu_e)$. KATRIN will thus be able to test the second input parameter of the Z-burst model, i.e. the rest mass m_{ν_i} of relic neutrinos. The independent tests by Auger and KATRIN should allow to verify or rule out the Z-burst model.

1.3 Particle physics

In this section we give an update on recent results from neutrino oscillation studies, focusing on the solar neutrino results obtained by the SNO experiment. We also discuss a claim for an evidence for neutrinoless double beta decay ($0\nu\beta\beta$), which -if verified- would indicate lepton number violation and the Majorana nature of neutrinos. Finally, we briefly discuss possibilities to measure CP violation in the lepton sector by combining results from $0\nu\beta\beta$ and β-decay searches.

1.3.1 Neutrino oscillations

The experimental evidence for ν-oscillations has been further strengthened by new solar neutrino results from the SNO experiment. Following initial results [23)] for charged current interactions $\mathrm{d}\,(\nu_e\,,\mathrm{e}^-\,\mathrm{p})\,\mathrm{p}$ of solar ν_e , the SNO Collaboration recently announced the result of the first *neutral current* measurement of ^{8}B solar neutrinos based on the observation of the deuteron breakup reaction $\mathrm{d}\,(\nu\,,\nu'\,\mathrm{n})\,\mathrm{p}$ [24)]. Assuming a standard ^{8}B-flux, the comparison of the neutral current rate with the charged current and elastic scattering rate allows to deduce a non-ν_e component $\phi_{\mu\tau} = 3.41^{+0.45}_{-0.45}(\mathrm{stat.})^{+0.48}_{-0.45}$ (syst.) $\times\,10^6\ \mathrm{cm}^{-2}\mathrm{s}^{-1}$ in the solar neutrino flux. This remarkable $5.3\,\sigma$ signal (from one experiment alone) gives strong evidence for ν_e flavour transformations and has solved the long-standing solar neutrino puzzle. It should be noted also that the total flux measured with the neutral current reaction is consistent with solar models.

In addition, the SNO Collaboration has released new data on the day and night solar neutrino energy spectra and rates [25)]. Measuring the day-night asymmetries of the neutral current, charged current and elastic scattering data, the first direct measurements of the day-night asymmetries of the ν_e-flux as well as of the total solar ν-flux were deduced. A global fit to these data strongly favours the so-called Large Mixing Angle (LMA) solution for matter-enhanced MSW (Mikheyev-Smirnov-Wolfenstein) transitions. Taking into account other solar neutrino results gives further support to this conclusion, so that at present the LMA solution is the only viable solution in the global oscillation analysis of solar neutrino data (all other solutions only appear for very high confidence intervals). The implications of this result for cosmology in general and for future tritium β-decay experiments in particular have been discussed above (see sect. 1.1.2).

1.3.2 Neutrinoless double beta decay

The detection of a neutrinoless double beta decay ($0\nu\beta\beta$) process would imply that neutrinos have Majorana type masses and that lepton number conservation is violated by two units (for recent $0\nu\beta\beta$ - reviews see [27,28]). At present, there are several experimental searches for $0\nu\beta\beta$ signals based on $\beta\beta$-unstable nuclei such as ^{76}Ge, ^{100}Mo, ^{116}Cd, ^{130}Te, ^{136}Xe and others. All experiments so far have yielded upper limits for the effective Majorana mass m_{ee} in the $\mathcal{O}$ (eV) range [27].

Evidence for neutrinoless $\beta\beta$ decay

The most sensitive $0\nu\beta\beta$ search has been the Heidelberg-Moscow experiment, operating five enriched high-purity ^{76}Ge detectors with a total mass of 11.5 kg in the Gran Sasso Underground Laboratory since 1990. A $0\nu\beta\beta$ signal $^{76}\mathrm{Ge} \rightarrow {}^{76}\mathrm{Se} + 2\,e^-$ would be based on the observation of a statistically significant peak in the Ge sum energy spectrum at the Q-value of $\beta\beta$-decay at $Q_{\beta\beta} = 2039$ keV. A previous analysis [29] based on data equivalent to 47.7 kg y has extracted an upper limit on the effective Majorana neutrino mass of $m_{ee} < 0.35$ eV (90 % CL.).

Recently, a new analysis of data corresponding to a measuring time of 54.98 kg y has been published [30]. Now, the existence of peaks around the signal region was assumed. Statistical techniques based on Bayesian and frequentist methods were applied to investigate the presence of a $0\nu\beta\beta$ peak at $Q_{\beta\beta}$. Restricting the analysis to a very narrow energy interval around $Q_{\beta\beta}$*, the peak finding algorithms indicate the presence of a weak signal with a statistical significance of $\simeq 2.2\sigma$ (for the Bayesian method). The authors of [30] use this result to claim an evidence for a signal from neutrinoless double beta decay. The signal extracted would correspond to a $0\nu\beta\beta$ half-life of ^{76}Ge of $T^{0\nu}_{1/2} = (0.8 - 18.3) \times 10^{25}$ y (95% c.l.) with a best value of 1.5×10^{25} y. For a specific set of nuclear matrix elements (h=1), this result translates into an effective Majorana neutrino mass $m_{ee} / h = (0.11 - 0.56)$ eV (95% C.L.), with a best value of $m_{ee} / h = 0.39$ eV. Here we have followed ref. [26] and introduced a normalization parameter h, which reflects the uncertainties of the nuclear matrix

*this procedure relies on additional and crucial assumptions on the nature of the background close to $Q_{\beta\beta}$

elements (h can vary from $0.6 \div 2.8$ for different calculations).

The conclusions and methods of [30] have been subject to criticisms recently [31,26]. The open issue of a $0\nu\beta\beta$ signal in [30] can however only be clarified by further experimental results, therefore a verification or refutation of this result is urgently required. If verified, this would imply the generic Majorana nature of neutrinos and, more importantly, the non-conservation of the lepton number. For the neutrino sector this would also imply nearly degenerate neutrino masses with masses in the sub-eV range, taking into account the small neutrino mass squared differences $\Delta m^2 \leq 10^{-2}$ eV^2 from global analyses of solar and atmospheric ν-experiments.

In the nearer future, new double beta decay results with a considerably improved sensitivity can be expected. Several ambitious experiments will investigate the parameter region of effective Majorana neutrino masses $\mathrm{m}_{ee} > 0.01$ eV with high precision. The use of different $\beta\beta$-nuclei and comparison of experimental results will allow to manifest a genuine $0\nu\beta\beta$ signal. However, the uncertainties of nuclear matrix elements for $0\nu\beta\beta$ decays will likely remain an open problem over the next years, rendering the precise determination of the fundamental ν-mass scale with $0\nu\beta\beta$ searches more difficult [27].

For these reasons, a high sensitivity direct measurement of the electron neutrino mass $\mathrm{m}(\nu_e)$ with a next generation tritium β-decay experiment is highly desirable. The KATRIN experiment will be sensitive to neutrino masses down to 0.35 eV (90 % CL.) which corresponds to the upper part of the parameter range suggested in [30]. Thus the results of KATRIN could either constrain this parameter range or precisely determine the mass scale, thereby contributing to the efforts to clarify the recent evidence for $0\nu\beta\beta$ from the Heidelberg-Moscow experiment. Moreover, in the case of a positive signal seen in future tritium β-decay and double beta decay searches, Majorana CP-phases could be investigated. This is discussed in more detail below.

Majorana CP-phases

Tritium β-decay results combined with data from $0\nu\beta\beta$ experiments could provide unique information on the CP-violation in the lepton sector of the Standard Model induced by so-called Majorana CP-violating phases [2,34,35,36]. For a quasi-degenerate neutrino mass spectrum with generic Majorana masses, a measurement of the electron neutrino mass $\mathrm{m}(\nu_e)$ from ^{3}H β-decay and of the effective Majorana neutrino mass m_{ee} from $0\nu\beta\beta$ could, in principle, give evidence for Majorana CP-violating phases, even though no CP-violation would be directly observed. This is due to the fact that m_{ee} depends on three parameters: the lightest neutrino mass eigenstate m_1 and the two CP-violating phases α_{21} and α_{31}.

Hence, the existence of CP-violation could be established by a precise experimental determination of the effective Majorana neutrino mass m_{ee} and the mass $\mathrm{m}(\nu_e)$ measured in tritium β-decay, taking into account independent precision measurements of the solar mixing angle $\theta_\odot$ and the mixing matrix element $|U_{e3}|^2$. These measurements would also imply a non-trivial constraint on the two CP-violating phases α_{21}

and α_{31}. For more detailed discussions of the reconstruction of the neutrino mass spectrum (quasi-degenerate, inverted, normal or partial hierarchy) and of measuring Majorana CP-phases we refer to [2,34,35]. In [37] an update is given on these issues, taking into account the latest SNO results.

2 Recent Results from Troitsk and Mainz

The tritium β-decay experiments at Mainz and at Troitsk have continued their neutrino mass measurements. In addition, both experiments have performed non-standard runs which have been dedicated to background investigations. In the following we give a summary of recent experimental results from Troitsk and Mainz.

2.1 The Mainz Neutrino Mass Experiment

2.1.1 2000 data

The Mainz Neutrino Mass Experiment finished the analysis of the 2000 data in 2001. These measurements were performed from October to the end of the year 2000 and consisted of the 2 runs Q9 and Q10. Between the two measurements a fresh T_2 film was prepared. The runs were performed by purpose under non-optimized experimental conditions concerning the preparation of the apparatus (i.e. no extra bake out). The idea was to check whether one could provoke a Troitsk-like anomaly (see sect. 2.2), which could also appear again at Mainz as being an experimental artefact. But no significant step-like anomaly was found. In particular, none was found in those two subsets of data which were obtained in parallel to data taking at Troitsk (December, 6-13 and December, 22-28). These synchronous measurements were performed to check a 'global' effect. In both periods Troitsk has observed significant steps [38], but with drastic changes in position and amplitude in between, which does not fit into the previous pattern of a half year period of the effect.

Although no step-like signatures in the latest runs Q9 and Q10 were found, most (not all) of the data subsets suffered again from small residual perturbations which resulted in negative $m^2(\nu_\mathrm{e})$ fit results in the range of -10 eV^2. Part of the data showed also a slight, but statistically significant hysteresis of the up- relative to the down-scanning of the spectrum. If charge trapping depends on the scanning direction, which is conceivable, then the resulting background events may well show a hysteresis. This problem disappeared or was washed out after introducing a random walk through the β-spectrum. The Mainz group ascribes the reappearance of slight spectral irregularities in the data to the then non-optimized status of the spectrometer. Although no indication for the appearance of any Troitsk-like anomaly was found, most of the data were not suited to give a solid result on the neutrino mass.

2.1.2 2001 data

To check whether the behavior of the Mainz Neutrino Mass Experiment in 2000 was indeed due to the not well-prepared situation, the Mainz group started another 3 month measurement campaign at the end of the year 2001. Before the measurements, a very careful maintenance and preparation of the whole setup was performed. Especially all parts which have to be refreshed from time to time were replaced. These were components related to the tritium source, the vacuum and the high voltage system (*e.g.* the graphite substrate, out-baking of all vacuum systems and re-activation of the non-evaporable getter pumps, the oil of the high voltage divider, and others). To check the various scanning hysteresis effects, different scanning methods were tested, including a 50 times slower scanning procedure. The summary of all these investigations is: the Mainz experiment has achieved its most stable operation mode ever in these two runs Q11 and Q12 of 2001. The background rate was about 13 mHz, lower than before and much more stable.

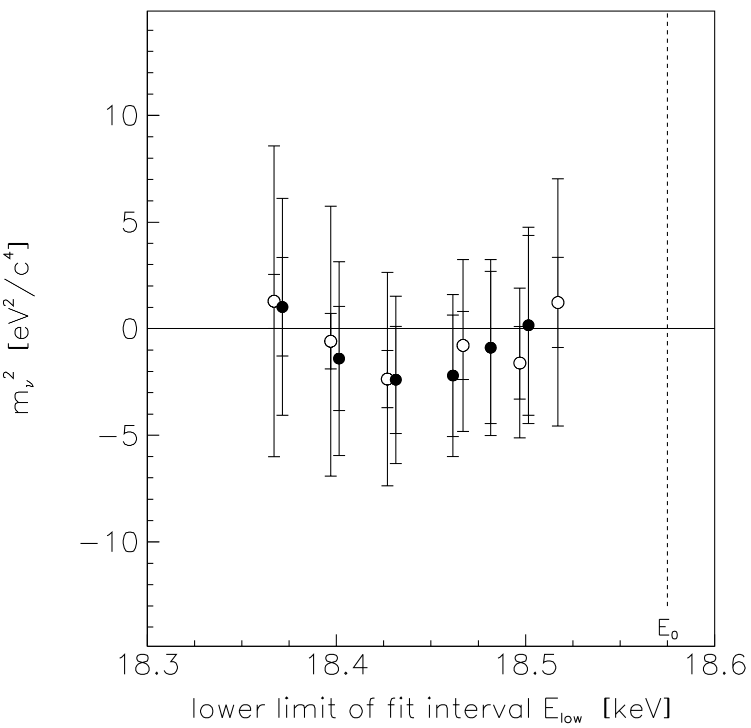

Figure 3: Mainz fit results on $m^2(\nu_e)$ as a function of the the lower boundary of the fit interval (the upper bound is fixed at 18.66 keV, well above E_0) for data from 1998 and 1999 [39] (open circles) and from the last runs of 2001 (filled circles) [40]. The error bars show the statistical uncertainties (inner bar) and the total uncertainty (outer bar). The systematic errors for large fit intervals with a lower boundary $E_{low} < 18.5$ keV are correlated.

The neutrino squared masses obtained from the fit are very stable and compatible with zero within their uncertainties and the previous Mainz results (see figure 3). No indication of a Troitsk-like anomaly or any residual problem in the Mainz data were found. A 4-parameter fit (neutrino mass, background rate, amplitude and end-point energy) to the 2001 data using the last 70 eV of the β spectrum below the endpoint gives a result for $m^2(\nu_\mathrm{e})$ of [40]:

$$m^2(\nu_\mathrm{e}) = +0.1 \pm 4.2 \pm 2.0 \ \mathrm{eV}^2 \quad \text{(for 2001)} \tag{2}$$

Combining this value with the one obtained from the data sets Q5–Q8 from 1998 and 1999 [39] gives

$$m^2(\nu_\mathrm{e}) = -1.2 \pm 2.2 \pm 2.1 \ \mathrm{eV}^2 \quad \text{(for 1998, 1999, 2001)} \tag{3}$$

which corresponds again to an upper limit [40] of

$$m(\nu_e) < 2.2 \ \mathrm{eV} \quad (95\ \%\ \mathrm{C.L.}) \tag{4}$$

The inclusion of the high-quality data from 2001 improves the Mainz sensitivity only marginally, showing that the Mainz experiment has reached its sensitivity limit (in this case, sensitivity is defined as the average limit one expects for a vanishing electron neutrino mass) .

At present, the Mainz group is installing a new electrode system to check new ideas to avoid background and to remove trapped particles.

2.2 The Troitsk Neutrino Mass Experiment

In 2001 and 2002 important experimental improvements were made to reduce and stabilize the background and running conditions:

- An additional differential pumping station was installed in between the gaseous tritium source and the spectrometer increasing the extinction factor of the pumping ports from 10^5 to 10^7. A new argon sputtering system was constructed to improve the cryo-trapping in between the gaseous tritium source and the spectrometer.

- A tritium isotope separator was installed which allows to keep the tritium concentration within the gaseous source at a level of $90-95$ % . This improvement increases the signal rate by a factor of 1.5 while using the same column density as in the previous measurements.

- The high voltage gradient between the spectrometer electrode and the grounded screen was reduced. This totally suppressed the formation of a spontaneous plasma, which was observed in previous starting periods.

- The spectrometer working temperature was lowered to $13-15°$ C, thus decreasing the background rate by a factor 3.

In total the background is now stable at a rate of about 10 mHz and does not increase anymore when opening the valve to the tritium source, similar to the Mainz experiment.

Between May 2001 and April 2002 three tritium runs have been performed. The May 2001 run does not show any spectral anomaly at a level above 1 mHz and resulted in

$$m^2(\nu_\mathrm{e}) = -5.5 \pm 6.5 \pm 2.0 \text{ eV}^2 \quad \text{(May 2001)} \tag{5}$$

The December 2001 run was very stable and had low background. The data show a small anomaly of an amplitude of (2.7 ± 0.5) mHz, which is at the lower end of the range of anomaly amplitudes observed at Troitsk so far. Considering this anomaly requires a 6-parameter fit procedure (with the additional parameters of a step position and amplitude). The fit gives

$$m^2(\nu_\mathrm{e}) = -5.2 \pm 6.7 \pm 1.5 \text{ eV}^2 \quad \text{(December 2001)} \tag{6}$$

The data from April 2002 are not analyzed yet.

Combining the 2001 results with the previous ones from 1994–1999 [41)] gives

$$m^2(\nu_\mathrm{e}) = -2.3 \pm 2.5 \pm 2.0 \text{ eV}^2 \quad (1994 - 1999,\ 2001) \tag{7}$$

from which an upper limit on $m(\nu_e)$ is obtained of

$$m(\nu_e) < 2.2 \text{ eV} \quad (95\ \%\ \text{C.L.}) \tag{8}$$

New data from both experiments will not improve the sensitivity on $m(\nu_e)$ significantly. This fact clearly underlines the importance of a next generation tritium β-decay experiment with a sub-eV sensitivity.

2.3 Spectral anomalies

All the Mainz observations leave little doubt that the residual spectral anomalies observed at Mainz in 2000 as well as in 1997 and early 1998 are of instrumental origin and related to the specific electrodynamics of MAC-E-Filters, and, moreover, that they can be overcome by paying utmost attention to UHV and surface conditions as well as to the electromagnetic design. Considering the non-existence of a correlation of the results of the parallel measurements at Mainz and Troitsk in 2000 and the facts that the anomaly at Troitsk did not follow an 0.5 y periodicity anymore in the year 2000 and that the anomaly seems to be much reduced in 2001 with the improved setup, it seems also very likely that the origin of the Troitsk anomaly is of instrumental origin.

3 The KATRIN experiment

In this section we give an overview of the current status of the KATRIN project and outline the progress in the design of key components of the experiment. For an

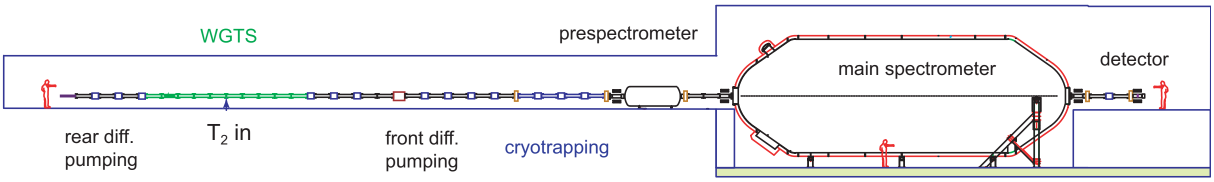

Figure 4: Side view of the KATRIN experiment in a linear configuration amounting to a beam line length of 70 m.

introduction to the initial design considerations of KATRIN and its electromagnetic layout we refer to our Letter of Intent [1]. The KATRIN experiment can be subdivided into the following major component (see fig. 4):

- two molecular tritium sources : a high luminosity gaseous windowless tritium source (WGTS) delivering 10^{10} β-decay electrons per second and a quench condensed tritium source (QCTS). Both sources will be used for alternate measurements with different systematic errors.

- an active differential pumping section at the rear and front side of the WGTS to reduce the flow of tritium molecules from the WGTS into the residual system and to guarantee a stable operation mode of the WGTS.

- a cryotrapping section with Ar-frost to eliminate the remaining flow of tritium molecules and to keep the spectrometer essentially tritium-free.

- a system of two electrostatic filters consisting of a pre-spectrometer at fixed retarding potential, which filters out low energy β-decay electrons and a large volume main spectrometer with an energy resolution of 1 eV to analyse the β-electrons close to the tritium endpoint at 18.6 keV.

- a segmented semiconductor detector or bolometer array to count the 18.6 keV β-electrons transmitted through the electrostatic filters.

3.1 Overview

The KATRIN experiment will be located on the site of Forschungszentrum Karlsruhe (FZK). At the time of submission of the LoI, the exact location of the experiment at the FZK site had not been fixed. Weighting the specific advantages and disadvantages of different hall options, we now have decided on a solution where the KATRIN experiment will be performed at the Tritium Laboratory Karlsruhe (TLK) (see fig. 5). The most significant advantage of choosing TLK as host laboratory for KATRIN is the possibility that the windowless gaseous molecular tritium source WGTS can be accommodated in the experimental zone B of TLK and be integrated into the tritium handling facilities of TLK (see below). This advantages make the TLK location the most cost effective solution for KATRIN.

The overall length of the KATRIN experiment amounts to $\sim$ 70 m for a linear configuration, which is strongly preferred by general electromagnetic design considerations [1)] (for an overview of the experiment see fig.4). This implies that only a part of the KATRIN experiment can be housed in the existing TLK building. Therefore, new buildings have to house the remainder of the KATRIN beam line, which extends a further 45 m in a straight line to the area north of TLK, which is a 'green field' site. Two lightweight steel construction halls are planned to house these parts of KATRIN, i.e. the cryotrapping part of the electron transport section, the QCTS and the two electrostatic spectrometers as well as the detector, electronics and DAQ. The existing TLK-building will be connected to the new KATRIN halls by two $2 \times 2\,\mathrm{m}^2$ openings fitted in the double wall structure of the TLK-building and equipped with an airtight sealing to prevent air circulation between the two parts of the experiment.

As shown in the detailed top view in fig. 5, the entire so-called inner tritium loop, consisting of the WGTS as well as the rear and front differential pumping sections (including the space for an electron gun) can be located within the experimental zone B of TLK. This close proximity of the WGTS and the general TLK infrastructure has the following advantages:

- the tritium inventory of KATRIN can be integrated into the certified tritium accounting scheme of TLK (only a single material balance area, MBA)
- the tritium supply to the WGTS at a rate of 10 g /day (see below) requires the infrastructure of TLK
- a short distance between the tritium supply and the WGTS maintains the high purity of tritium and ensures safe handling procedures
- tritium recovery and treatment of gaseous wastes at TLK is straightforward
- the existing air circulation system of TLK can be used by KATRIN with regard to safety and operation aspects

3.2 Tritium Sources

The KATRIN experiment will make use of two molecular sources: a windowless gaseous tritium source (WGTS) and a quench condensed tritium source (QCTS) for alternate measurements with different systematic errors. The WGTS will be the standard source used for the long-term tritium measurements as it offers the highest luminosity. Apart from the standard tritium measurements, specific modes of operation of the WGTS will be required from time to time. The different modes of tritium source operation are listed below:

- standard operation of the WGTS
- standard operation of the WGTS in the ToF mode

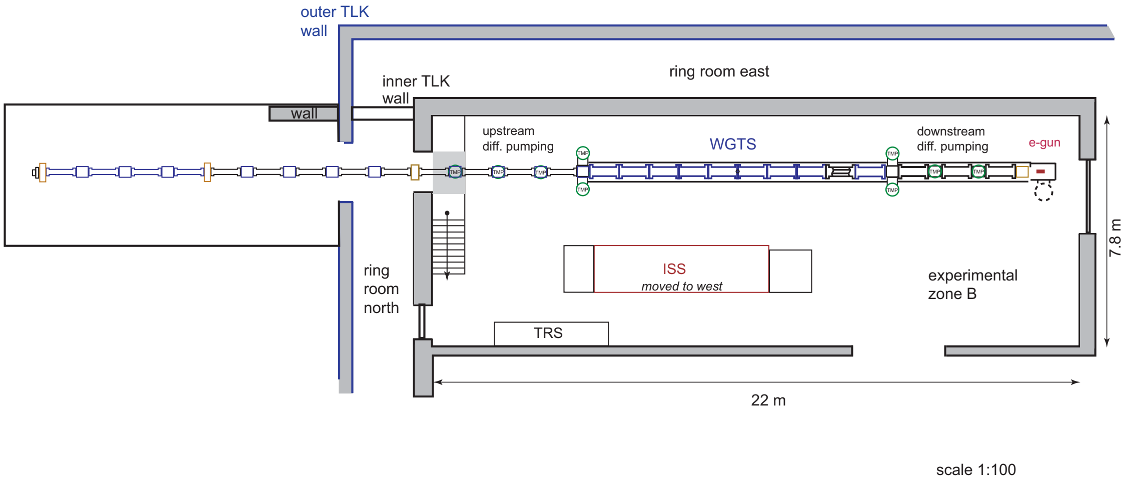

Figure 5: Top view of the WGTS and the rear and front differential pumping sections located at the experimental zone B of Tritium Laboratory Karlsruhe.

- energy calibration with gaseous ^{83m}Kr
- measurement of the WGTS work function with ^{4}He
- energy loss measurements of 18.6 keV electrons in WGTS
- QCTS operation
- source system cleaning by bake out
- source system cleaning by glow discharge

These different modes are discussed in more detail in the following and specific parameters required for the operation of particular modes are.

3.2.1 Standard operation of the WGTS

The standard operational mode of the WGTS will be the long-term measurement of the T_2 integral spectrum in the region close to the β-endpoint at 18.6 keV. More than 75 % of the entire measuring time with KATRIN will be allocated t this mode. Single tritium runs will last for approximately 50-60 days with an estimated average of 4 runs per year. A net measuring time of about 1000 days in this mode is required to achieve a neutrino mass sensitivity of 0.35 eV [1)].

In this operation mode the tritium β-spectrum is measured by scanning the potential difference between the tritium source and the analyzing plane of the main spectrometer. For this purpose the source potential will be swept from 0 V to − 100 V and the main spectrometer voltage will be kept at the fixed value of − 18.6 keV with a demand on the stability level of a few ppm. In the WGTS, pure molecular tritium with a T_2 content of more than 95 % and an isotopic stability of better than 1 % will be circulated. The source temperature will be adjusted to a specific value within the operational range from $28-32\,\mathrm{K}$. To avoid tritium density changes in the source, this temperature value has to be stabilized to a precision of about $1\,\%$. The T_2 molecules will be injected by a capillary at the middle of the 10 m long tritium tube with an injection rate of 10^{19} molecules per second, corresponding to 0.37 cm^3/s (STP) or 0.95 Ci/s. This throughput corresponds to about 10 g of tritium per day. This rate has to be compared with the actual inventory of the TLK for 20 g and the license of 40 g. The injection rate has to be stabilized at the $1\,\%$ level. The WGTS column density will be 5×10^{17} cm^{-2} with a central T_2 pressure of 4×10^{-3} mbar at $30\,\mathrm{K}$.

3.2.2 Standard operation of the WGTS in ToF mode

This operation modus of the WGTS will be identical to the standard mode of operation except for the following important modification: the source potential will be pulsed with 100 V_{pp} to simultaneously measure the ToF of the β-electrons from the source to the detector. The length of single pulses will be in the μs range which will allow to perform a differential measurement of the tritium β spectrum. The ToF measurements will be focused on systematic studies and background investigations, requiring measurement times of the order of $10-20$ days per year.

3.2.3 Energy calibration with gaseous ^{83m}Kr

An absolute calibration of the energy scale of the main spectrometer can be carried out using conversion electrons from gaseous $^{83m}\mathrm{Kr}^{\dagger}$. The most important calibration line will be the K-32 line at an electron energy of 17.8 keV (FWHM 2.8 eV), other lines of interest will be the L-32 lines at 30.4 keV and the N-32 conversion lines at 32.1 keV (see also section 3.8.1).

The modifications required for this mode are the following: small amounts of gaseous ^{83m}Kr from a Rb/Kr emanation source have to be added to the tritium gas at an appropriate partial pressure. It is planned to work with a krypton-tritium ratio of the order of 10^{-6}. The added Kr-gas would require a higher WGTS temperature of $100-150\,\mathrm{K}$. In this temperature regime, the source profile of the WGTS could be mapped by the ^{83m}Kr measurements and be compared to calculations. In addition, possible electrostatic field effects caused by trapped charges or voltage shifts due to tritium adsorption on the inner tube walls could be investigated.

To measure the conversion lines from ^{83}Kr together with the underlying tritium β-spectrum, the source potential will be varied in the range from $0\,\mathrm{V}$ to $-100\,\mathrm{V}$. The spectrometer potential will be adjusted to voltage values corresponding to the conversion electron lines, i.e. to -17.8 kV for the K-32 conversion line and to -32.1 kV for the N-32 lines. For the K-32 line measurements this implies that the detector (see sect. 3.7) has to be able to handle a high rate of β-electrons from the last 800 eV

†a second independent ^{83m}Kr source, condensed onto a cold backing for long-term monitoring of the spectrometer HV is discussed below in sect. 3.8.2

of the tritium spectrum and the other ^{83m}Kr conversion lines. The ^{83m}Kr calibration will be performed before and after single tritium runs ($50-60$ days) and will take up to several hours in continuous operation.

3.2.4 Measurement of the work function with ^{4}He

The retarding energy of the KATRIN spectrometer can be accessed for calibration and monitoring purposes by performing the following two precise measurements:

1. A measurement of the applied high voltage using a high precision HV divider and a high precision digital voltmeter or a comparison of the divided voltage to a voltage standard.

2. The measurement of the difference of the work functions of the source and the spectrometer (compare to equation 12).

Currently we investigate the possibility to measure the difference of the work functions by high precision spectroscopy of a very sharp electron line at 35 eV originating from an auto-ionization state of ^{4}He with the KATRIN spectrometer (see sect. 3.8). As the absolute energy resolution ΔE of a MAC-E-Filter scales with energy as $\Delta \mathrm{E} = \mathrm{E} \times (\mathrm{B_{min}}/\mathrm{B_{max}})$, at an energy of 35 eV the energy resolution of KATRIN will be of the order of 2 meV. These measurements would require significant modifications of the source operation mode, in particular, they would require the total removal of T_2 from the source system by cooling to LHe temperature. Instead, the WGTS would be filled with ^{4}He gas (with an added carrier gas). The stability of the ^{4}He-gas density has to be better than 10 %. The tolerable amount of He-gas which is adsorbed onto the inner tube surface of the WGTS during these measurements is still under discussion (this is a function of the tube temperature).

The excitation of the ^{4}He atoms in the WGTS will be by electron impact, using electrons from an electron gun with currents in the pA-range. The e-gun will be operated in pulsed mode with single pulse times of the order of 1 μs. To reflect the initial electron pulse with energies of a few hundred eV from the e-gun, the retarding potential of the pre-spectrometer will be ramped up synchronously. The reflected pulse will generate the low-energy electrons from the ^{4}He auto-ionization. To transmit these 35 eV electrons to the main spectrometer, the pre-spectrometer retarding potential has to be ramped down in time. The energy of the transmitted electrons is then measured by sweeping the source potential from 0 V to -10 V while keeping the main spectrometer voltage at a fixed voltage of about -35 V. The measurement of the difference in the work functions will take up to several days in continuous operation with 1-2 measurements planned over a calendar year.

3.2.5 Energy loss measurements of 18.6 keV electrons

The measurements of the energy losses of 18.6 keV electrons in gaseous tritium are intended to obtain an energy loss spectrum as well as to determine the total inelastic cross section of electrons at this energy. The cross section measurement is important to describe the scattering processes of β-electrons in the WGTS. The cross section uncertainty (currently $\simeq 2\,\%$) is the parameter which will dominate the systematic error in the KATRIN measurements[‡].

The parameters of the WGTS during this type of measurements will be identical to the standard mode of operation. Mono-energetic electrons from an electron gun will be injected into the rear part of the WGTS source tube with a frequency of several kHz. The stability of the electron gun has to be better than 10^{-3} to allow a precise measurement of the integral energy spectrum of 18.6 keV electrons. From the technical point of view, the energy loss measurements will be carried out by keeping the source at ground potential (0 V) while at the same time varying the electron gun voltage by $\Delta U = \pm\,150$ V around a central value of 18.6 kV. A sufficiently precise measurement of the inelastic electron cross section will require a measurement time of several days.

3.2.6 QCTS operation

The QCTS operation will be alternate to the WGTS operation and a comparison of the results from both sources should allow to investigate systematic effects in the KATRIN measurements. To measure the integral tritium β-spectrum close to the endpoint, the QCTS source potential will be swept from 0 V to $-$ 100 V and the main spectrometer voltage will be kept stable at -18.6 keV. Details of the QCTS set-up have already been reported in the KATRIN LoI [1)].

Currently we are investigating the problem of self charging of the frozen source, which up to now is a cause of systematic uncertainties in the measurements with the QCTS. These investigations [42)] will be of crucial importance for the use and the allocated measurement time of the QCTS in the KATRIN experiment.

3.2.7 Source system cleaning by bake out

The initial cleaning and outgassing of all relevant inner surfaces of the tritium source and the electron transport section will rely on the bake out at high temperatures (vacuum pumping at high temperature). For the WGTS a bake out temperature of 500 K will be required, whereas the differential pumping section will be heated up to 400 K and the cryogenic sections to 500 K. This bake out procedure will have to be repeated after some time to remove tritium and argon from the inner surfaces.

3.2.8 Cleaning the transport system by glow discharge

A glow discharge in H_2 or D_2 leads to an exchange of the isotopes adsorbed at the inner surfaces. For short transport elements of the order of 1 m this effect can be used

[‡]the scattering of electrons in the WGTS becomes important if an energy interval larger than 20 eV below the β-endpoint is analyzed [1)].

to reduce the amount of T_2 in the system. This option is still under discussion.

3.2.9 Source summary and future options

The safe and stable operation of the tritium source(s) in the different modes outlined above will be technologically challenging. A particular challenge will be associated with the required stability in the operation of the WGTS: not only the tritium and other gaseous compositions have to be stabilized (requiring an injection of about 10 g of high purity of tritium per day) but also the temperature needs to be controlled over a broad range.

Finally, we would like to mention that we are currently investigating methods and possibilities for Laser Raman real-time measurements for the WGTS. Spontaneous Raman spectroscopy using laser excitation is well suited to provide real-time quantitative analyses of chemical compositions in gas mixtures. Laser Raman spectroscopy is particularly advantageous for monitoring mixtures of hydrogen isotopomers containing tritium and deuterium because of its excellent differentiation among species. This technique has been developed and successfully tested at TLK [43] and should allow to monitor the gsd composition in the WGTS in-situ, thereby contributing to the minimization of the systematic effects during the long-term measurements.

3.3 Electromagnetic Design

After fixing the principle electromagnetic design parameters of the KATRIN experiment [1], three questions have been addressed in more detail recently:

- The background from the tritium sources and the spectrometers
- Adiabatic transport conditions
- The detailed design of the pre-spectrometer.

3.3.1 Background from trapped particles

The Mainz and the Troitsk set-up are currently used to study background and to check new ideas for the KATRIN experiment in order to avoid or to reduce background sources [44] (see also sect. 2).

From the Mainz experiment we have strong indications that trapped particles in the spectrometer play an important role with respect to the background. This is based on the following two observations. Firstly, after a change of the experimental conditions the background rate changes with time constants of up to about thousand seconds [45]. Secondly, under unfavorable experimental conditions there appeared hysteresis effects which depend on the scanning direction or on the residual gas pressure [44,46]. Since KATRIN plans to use a much larger spectrometer volume but aims for the same background rate, special emphasis has to be put on trapped particles, i.e.

one has to avoid them or at least to remove them to explain the background from the spectrometers by stored electrons or – what is less likely for the present spectrometers – by stored protons, various two-step or three-step processes have to be considered.

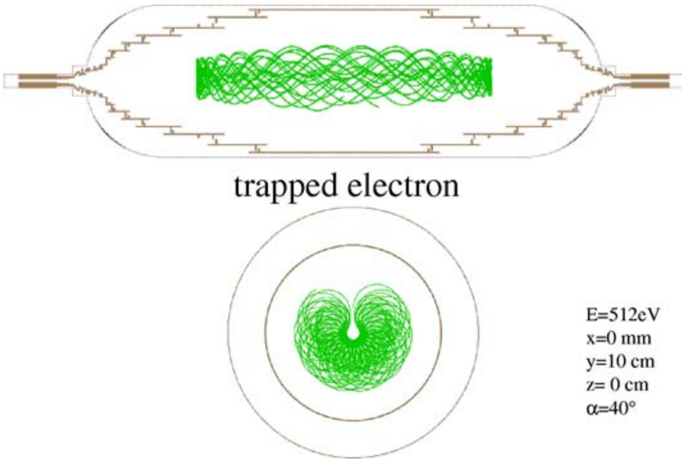

Figure 6: Example for a stored electron inside the Mainz spectrometer, for details of the starting conditions see the numbers given in the figure. The electron is stored axially by the magnetic field and longitudinally by the magnetic field gradient ("magnetic mirror"). A slow rotation around the symmetry axis, the magnetron drift, is visible, which is due to the curvature of the magnetic field (see curvature drift (11)) and a not completely vanishing transversal component of the electric field (see $\vec{E} \times \vec{B}$ drift (9)).

The trapping of particles has been studied in more detail by Monte Carlo simulations. In addition to the commercial program "Simion 7.0" the program "Adipark" was developed [47], which tracks only the guiding center of a gyrating particle to allow faster simulations. To check the long-term behavior, also the adiabatic drifts to first order were taken into account:

$$\vec{E} \times \vec{B} \text{ drift} \qquad \vec{u}_E = \frac{c}{B^2} \vec{E} \times \vec{B} \tag{9}$$

$$\text{gradient drift} \qquad \vec{u}_G = -\frac{cE_\perp}{eB^3} \vec{B} \times \nabla_\perp \vec{B} \tag{10}$$

$$\text{curvature drift} \qquad \vec{u}_C = -\frac{2cE_\parallel}{eB^3} \vec{B} \times \nabla_\perp \vec{B} \tag{11}$$

For low-energy electrons new possible Penning traps in the corners of electrodes were identified. Electrons with energies of a few eV up to a few keV can be stored by the magnetic mirror effect in the spectrometer. Sometimes also the electric retarding potential plays a role. Figure 7 shows the calculated "trapping volume" of electrons started with 16 eV in the Mainz spectrometer. Any electron which starts inside the contour lines under an angle with respect to the local magnetic field line, which is larger than the value specified for this contour line, will be trapped.

To remove stored electrons, the transversal drift terms of adiabatic motion in first order can be used. For the case of a MAC-E-Filter it is much more efficient to apply

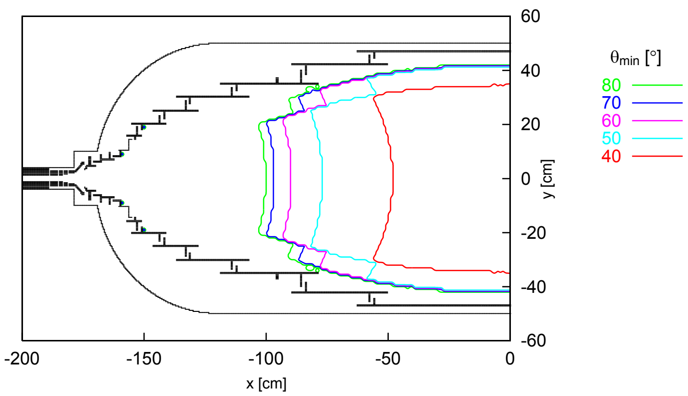

Figure 7: Trapping volume for electrons with a start kinetic energy of 16 eV calculated for the Mainz spectrometer.

a perpendicular electric field $\vec{E}$ and to use the $\vec{E} \times \vec{B}$ drift (9) than to bend the spectrometer and to use the curvature drift (11), an idea also discussed earlier for KATRIN. Figure 8 shows how the trapping condition for the example of figure 6 is cancelled by a transversal electric field composed of a central dipole electrode within the Mainz spectrometer.

In principle this method should work fine and remove stored electrons even using tiny transversal electrical fields only, if the magnetron motion (see figure 6) would not stabilize the motion of the trapped particle. Therefore the trapping condition is violated only for electrical fields above a certain value. A good estimate is that the $\vec{E} \times \vec{B}$ drift has to be faster than the velocity of the stabilizing magnetron motion. The program "Adipark" was used to study this in more detail. Figure 9 shows the strongly reduced trapping volume for 16 eV electrons calculated for the Mainz spectrometer with the applied electric dipole.

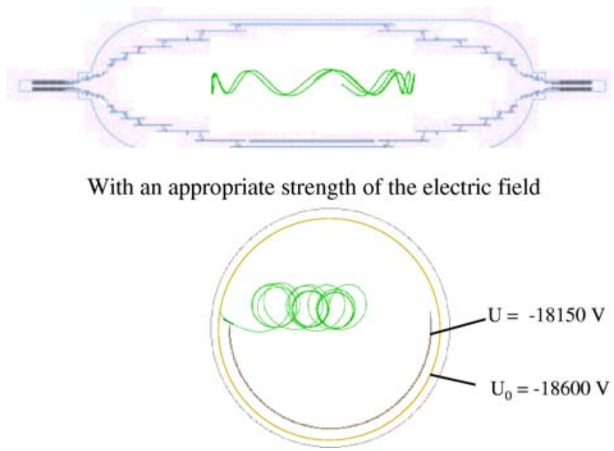

Figure 8: Cancellation of the storage condition for the trapped particle of figure 6 by a perpendicular electric field.

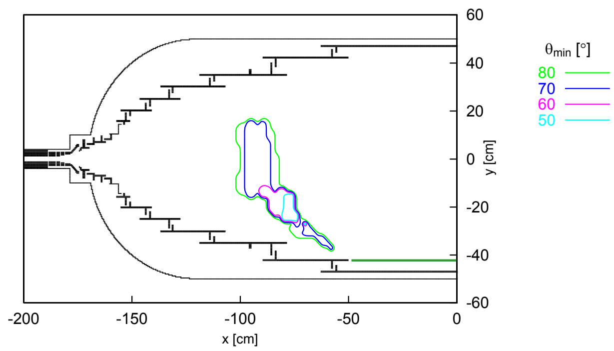

Figure 9: Trapping volume for electrons with a start kinetic energy of 16 eV calculated for the Mainz spectrometer with the applied electric dipole.

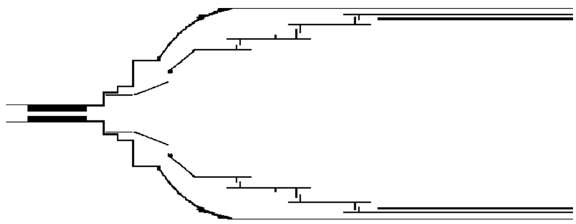

Figure 10: New Mainz electrode system with active electric dipole electrodes to remove stored electrons.

With the help of these calculations a new electrode system including several dipole electrodes to remove stored particles was designed for the Mainz spectrometer (see figure 10) [48]. The Mainz spectrometer was dismounted in early 2002 and equipped with this new electrode system (see figure 11) to check these new ideas for the KATRIN experiment. The start of these experiments is expected in June 2002.

Studies on the influence of trapped particles in local magnetic field minima in the pumping ports of the electron transport system are under way. Here the life-time of trapped particles is limited by elastic and inelastic scattering processes, the emission of synchrotron radiation and the curvature drift (11). An upgrade of the program "Adipark" to incorporate the latter two processes is in progress.

Another topic under investigation is to find methods to reduce the possibility of electron trapping in the Penning-like trap between the pre- and the main spectrometer of KATRIN. Here, different ideas like transversal electric fields or curved magnetic fields are currently studied by simulations.

3.3.2 Ideal adiabatic transport conditions

With the microscopic tracking programs "Simion 7.0" and "Partopt" the adiabatic transport conditions are investigated. After first checks of the adiabaticity inside the KATRIN main spectrometer [49] the influence of the many magnetic bends in the electron transport system was investigated, showing that they produce a significant

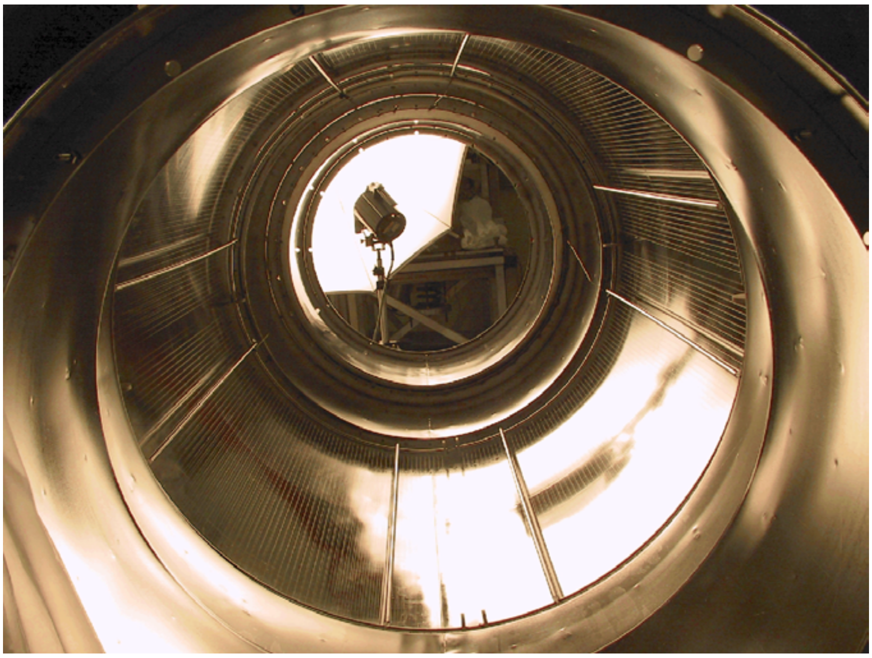

Figure 11: The upgraded electrode system of the Mainz spectrometer with its new central dipole electrode. The wire-based electrode was built in April/May 2002.

violation of the adiabatic energy transformation[51)]. Microscopic particle tracking through the whole setup including synchrotron radiation is under way.

A special question which is currently investigated is the minimum magnetic field strenght at any point which is possible without violating adiabaticity. Smaller magnetic fields reduce slightly the costs of the superconducting magnets, reduce the trapping of protons and the electron energy losses due to synchrotron radiation, but have potential disadvantages, like the enhanced sensitivity to stray fields or the violation of adiabatic transport. In the LoI of the KATRIN experiment [1)] an overall scaling factor of $0.6 \leq f \leq 1$ was given, which is safe with respect to these items.

Influence of ferromagnetic materials on the low magnetic field area in the main spectrometer

The INTMAG Code is used to calculate the influence of ferromagnetic materials (e.g. construction steel) on the magnetic field in the main spectrometer centre area. As the code is essentially 2 dimensional only radially symmetric distributions of high μ materials around the main tank can be investigated. First simulations for large structures with a relative $\mu < 1000$ (The DIN VDE 0185 TEIL 104 gives $\mu = 200$ for construction steel) and a distance of at least from the tank surface indicate small effects which can be compensated by external coils.

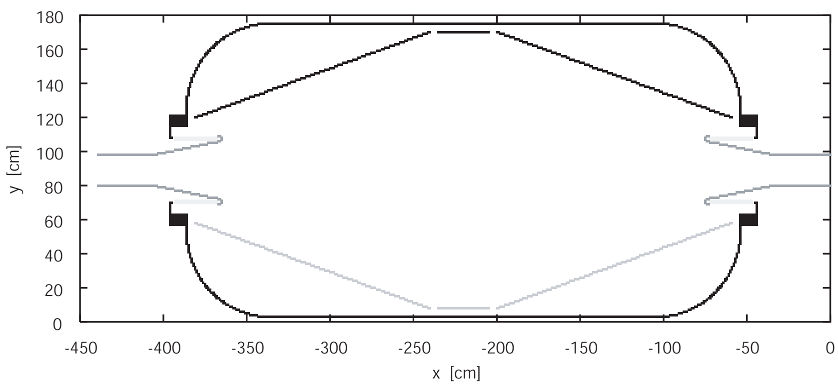

Figure 12: Optimized electrode configuration of the KATRIN pre-spectrometer. The different parts are at retardation voltage (black), insulators (light gray), and at ground potential (dark gray). The dipole electrode (medium gray) have the task to remove stored particles.

3.3.3 Pre-spectrometer design

A detailed electromagnetic design study for the pre-spectrometer was done to address several items:

1. The magnetic fields and magnet parameters should guarantee the requirements on energy resolution ($\Delta E \leq 50$ eV), the transportation of the whole magnetic flux§, and a smooth magnetic gradient to fulfill adiabaticity.
2. The electric design should provide a reasonably small electric potential inhomogeneity ($\Delta U \leq 50$ V) and application of the high voltage to the vacuum vessel.
3. The design of the electric and magnetic fields should avoid the possibility of local discharges (large distances, large radii of curvature of electrodes, no nearby surfaces at different potential connected by magnetic field lines, ...).
4. The investigations mentioned in section 3.3.1 were also applied to the pre-spectrometer design to avoid traps in the “corners” of the electrodes ($\Rightarrow$ shaping electrodes in the corners) and to design a system of dipole electrodes for active trap cleaning.

To fulfill these items and to build a set-up which is as simple as possible, a 0-electrode design is proposed. In this case the vacuum vessel is at high potential and provides the retardation. To remove trapped particles this set-up is equipped additionally with 3 pairs of dipole electrodes (see figure 12).

§Also considered was the new idea to transport the full electron flux emerging from the WGTS to the end of the pre-spectrometer. This would allow to install a flux monitor there for counting of β-electrons at the upper end of the β-spectrum. This monitor would be sensitive to the actual setting of the retarding voltage.

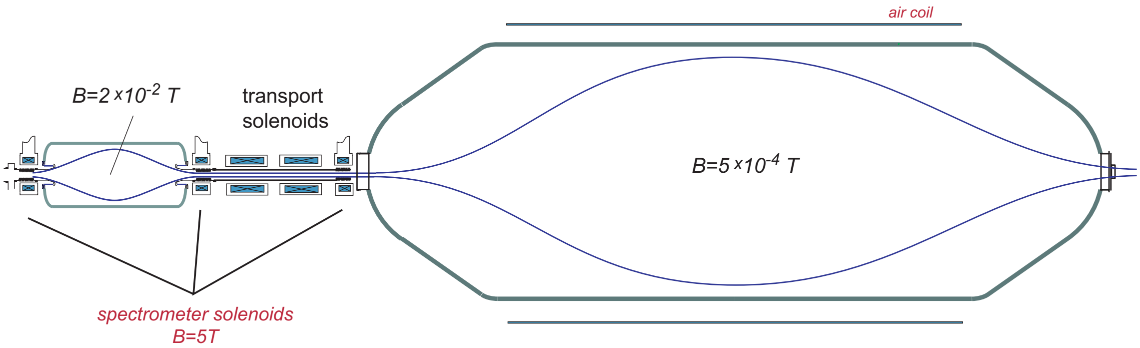

Figure 13: The electrostatic filter system of KATRIN consists of a pre-spectrometer working at a fixed retarding potential just below the retarding potential of the main spectrometer which is followed by a large main spectrometer with 1 eV energy resolution. Both spectrometers are connected by two superconducting transport solenoids which are tilted relative to each other to prevent a direct line of sight.

3.4 Electrostatic Spectrometers

The electrostatic filter system of KATRIN consists of two retarding spectrometers: a pre-spectrometer working at a fixed retarding potential relatively close to the end-point of the β-spectrum but low enough to make sure that background from the pre-spectrometer cannot pass the main spectrometer and a high resolution main spectrometer with a diameter of 7 m and a length of 20 m for the scanning of the tritium β-spectrum close to the endpoint. Both spectrometers are connected by two 1 m long super-conducting transport magnets.

The pre-spectrometer rejects the majority of β-electrons. The task of pre-filtering of β-electrons requires only a rather limited energy resolution of 50 eV for the pre-spectrometer. This fact considerably relaxes the demands with regard to the homogeneity of the magnetic field strength and electrostatic potential in its middle plane. The reduced rate of β-particles suppresses the background rate from ionising collisions with residual gas in the main spectrometer. The main spectrometer will have an energy resolution of 1 eV for final energy analysis of β-electrons.

For both spectrometers, very stringent XUHV conditions are required with final pressures below 10^{-11} mbar (see sect. 3.5). It will be a major technological challenge to achieve these XUHV conditions in large volume recipients. Therefore, we plan to investigate material selection criteria, different manufacturing processes as well as various surface treatment procedures in a multi-step construction schedule: at first, prototype tests will be carried out with a smaller size UHV test cylinder. This initial test phase will be followed by the construction of the mid-sized pre-spectrometer, before finally the large volume main spectrometer will be built. Each UHV recipient will be regarded as a *test bed* for the subsequent larger recipient and experiences gained during the extensive vacuum tests with each recipient will be used in the later phases of the project to optimize the construction work. In the following we report on the actual status of these investigations.

3.4.1 UHV prototype tests

In a first step the test recipient, a cylindrical tube with a length of 1.42 m and an outer diameter of 0.52 m (see fig. 14). Its geometry is identical to the pumping tubes of the pre-spectrometer (see fig. 15) was built. At each end a 500 mm flange is mounted to the cylindrical body. The counter-flanges have an endcap welded into the flange-ring with several smaller flanges attached to it for turbomolecular pumps and vacuum gauges. As the test vessel has been manufactured from the same stainless steel batch as is planned for the pre-spectrometer, the experiences gained can directly be transferred to the later construction of the pre-spectrometer and help to define reliable and reproducible test procedures for quality assurance.

Figure 14: The UHV test cylinder manufactured at DWE upon arrival at FZK. The vessel is equipped with stainless steel pipes welded to the surface for circulating a heating and cooling oil.

Currently, the test vessel is being fitted with a thermal insulation and a high compression turbomolecular pump (TMP) is mounted to the flange. After initial leak tests, the 500 mm flanges will be sealed by one Helicoflex gasket, which requires a well defined surface roughness for proper sealing. In the final configuration the 500 mm flanges will be equipped with a double sealing by two Helicoflex gaskets and a fore-vacuum of 10^{-3} mbar in between.

In the following we give an overview of the test schedule which has been worked out for the UHV test cylinder. The main objectives of these tests are:

- Measurement of the final pressure that can be reached with TMPs
- Measurements with gradually increased baking temperatures of the test cylinder from 150°C up to 350°C
- Pumping tests with additional NEG-getter strips in the cylinder

- Test of surface coating techniques to reduce outgassing

The corresponding test schedule for the pre-spectrometer will be adapted and optimized taking into account results from the test cylinder.

3.4.2 Pre-Spectrometer

The pre-spectrometer (fig. 15) will be a cylindrical tank with a length of 3.42 m long and an inner diameter of 1.70 m. These dimensions have been fixed by the electromagnetic design (see sect. 3.3) yielding an optimized electrode system and an optimum distance of the spectrometer magnets. Two cylinders with a diameter of 50 cm will be attached to the vessel at a longitudinal distance of 0.75 m off centre, leaving enough space for an optional air coil. The shorter cylinder will serve as a port for vacuum gauges. The longer cylinder will be used as a pumping port, with a VAT CF 200 all-metal valve and TMPs mounted on the lid and NEG-getter strips arranged inside. The length of the pumping port is determined by the maximum magnetic field tolerated by the TMPs. The vessel walls are 1 cm thick and are made of 1.4429 (316 LN) stainless steel.

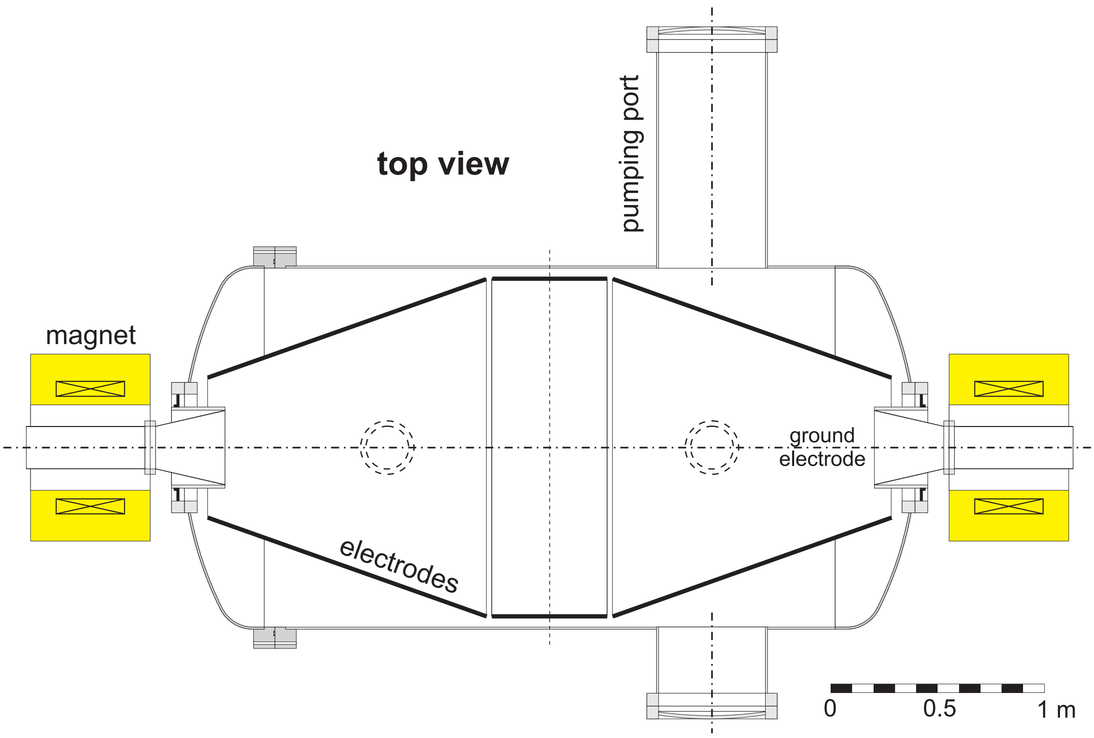

Figure 15: The KATRIN pre-spectrometer is a 3.42 m long steel vessel with a diameter of 1.7 m which is equipped with a system of inner electrodes for field shaping and suppression of background.

There will be three different types of flanges on the pre-spectrometer:

- At the endcaps and at the pumping ports flange rings with an inner diameter of 500 mm, an outer diameter of 610 mm and a height of 60 mm will be used. They are made of 1.4429 (ESU) stainless steel with low inclusion content. Flange rings welded to the tank have a flat sealing surface. The counter flanges have a groove holding two Helicoflex gaskets. Two holes connecting the space in between both gaskets will be connected to a vacuum-pump (via DN 16 KF), allowing to maintain a fore-vacuum of about 10^{-3} mbar.

- For smaller flanges commercially available flange rings will be used, ranging from DN 40CF to DN 200CF.

- Detailed parameters of a large tank flange with an inner diameter of 1.7 m have yet to be defined. It will be used to introduce and mount the electrodes.

All inner surfaces will be electro-polished. Further metallic coatings to reduce H_2 outgassing or pump H_2 actively (NEG getter coating) will be investigated with the test cylinder.

The form of the electrodes resulting from the current electromagnetic design of the pre-spectrometer still allows different options for details in shape, material and mounting. The layout shown in fig. 15 has two conical sections and a straight cylinder in between. All sections are electrically subdivided into two halves. One half of the electrode system will be permanently at the retarding potential, the other half can be pulsed down repeatedly with an amplitude of about +1000 V, removing trapped electrons.

The electrodes have to have openings for vacuum pumping. Using less material also helps to reduce outgassing. Stainless steel electrodes could either be in the form of perforated sheet metal, or a wire mesh. It has also been suggested to use aluminium because of its low hydrogen outgassing rate. In addition the low Z produces fewer cosmic ray or gamma induced electrons.

Different types of electrodes and material are currently tested with the Mainz spectrometer. It is also possible that a different electrode design will have to be tested in the pre-spectrometer if initial results are unsatisfactory. The mechanical design of the electrodes will be done at FZK. It is planned that the electrode system will be assembled outside of the vessel and inserted as a whole through the large flange.

Currently we are finishing work on a design proposal for the pre-spectrometer which will give further details on the experimental set-up as well as on the measurement programme and will serve as the basis for the soon to be started construction of the pre-spectrometer.

3.5 Vacuum system

The vacuum system of the entire KATRIN beam line can be subdivided into the following three sections:

- the active differential pumping section
- the cryogenic pumping section
- the XUHV system of the pre- and main spectrometer

Each pumping section has to fulfill specific tasks and faces technological challenges which will be outlined in more detail below.

3.5.1 Differential and cryogenic pumping

The differential pumping system of the WGTS is located both at the rear and front end of the tritium tube (see fig. 5), the cryopumping section is located upstream of the pre-spectrometer. The differential pumping section has to be designed so that molecular tritium of very high purity is circulating under stable conditions in the WGTS. Of equal importance is the minimization of the outflow of tritium molecules after the last active pumping port. The cryogenic pumps have to safely trap the remaining tritium flow after the active pumping section, i.e. to safely exclude the penetration of T_2 into the spectrometer section. Moreover, it is required that the migration of T_2 molecules is minimal even after warming up of the system, i.e. one has to provide means to very efficiently clean the system.

The layout of the KATRIN vacuum system will be based on the design of the UHV systems in Mainz and Troitsk [1)]. Both experiments have also developed efficient cleaning procedures for their spectrometers in case of migration of T_2 molecules in trace amounts into the spectrometers. For the KATRIN system, the amount of T_2 present at a given point under standard operation is well known and will be continuously recorded in the active differential pumping system. In the case of an increase of the tritium flow to a non-acceptable level, a computer-controlled guard valve in front of the cryogenic pumps will be closed. To prevent T_2 migration into the cryogenic system, the temperature has to be kept below a well-defined value. In case of a warm up, the gate valve to the pre-spectrometer will be closed and the cryogenic pumps will be cleaned.

The flow of tritium into the cryogenic pumps adjacent to the active pumping section results in covering this part of the system with a few monolayers of T_2 (the maximum permissible total load is $< 1\,\mathrm{Ci}$, corresponding to about 1 monolayer on one m^2). The downstream end of the cryopumping section pointing to the pre-spectrometer will be essentially free of tritium as long as the whole system is kept at the nominal operating temperature. After warming up, the T_2 will begin to migrate. To prevent the T_2 molecules from distributing randomly, they will be condensed on Ar snow. In the warming-up phase, the T_2 will be blown out through the upstream end of the cryotrapping section by a stream of He. The remaining traces of T_2 will then be removed by baking the system at $500\,\mathrm{K}$.

3.5.2 Spectrometer XUHV system

The challenges for the XUHV system of the pre- and main spectrometer are related to the following topics:

- the large dimensions of the main spectrometer vessel, causing problems in manufacturing (welding etc.) and surface treatments
- the required partial pressure of tritium, which is well below the detection limit of the best quadrupole mass filters
- the required final XUHV pressure below 10^{-11} mbar for large recipients

The stringent XUHV conditions required in both spectrometer vessels are closely related to the suppression of background processes. For the pre-spectrometer, the main problem arises from ionising collisions of electrons from tritium decay with the residual gas. The WGTS operating under standard conditions (see sect. 3.2.1) will deliver a rate of about 10^{10} β-electrons with energies up to 18.6 keV which are guided to the pre-spectrometer. At a pressure of 10^{-10} mbar the expected rate for ionising collisions is about 100/s. These electrons can get trapped, however, electrons stored in the pre-spectrometer volume do not *directly* cause an increase of the background rate, as these electrons cannot pass the main spectrometer retarding potential. However, taking into account the secondary interactions of ions produced in these ionizing collisions, there are several multi-step processes which could lead to an increased background rate in the main spectrometer. Therefore, stringent XUHV-conditions with a total pressure of less than 10^{-11} mbar are required for the pre-spectrometer. Moreover, as outline in sect. 3.4, the pre-spectrometer will act as a *test bed* for the larger main spectrometer during the construction phase of KATRIN, and will be used to investigate and optimise XUHV-techniques.

Of major concern for the background rate will be tritium molecules decaying in the main spectrometer. These β-decays will result in high energy keV decay electrons that will be trapped in the magnetic bottle formed by the spectrometer magnets. More dangerous, however, will be the accompanying low-energy shake-off electrons, which are emitted in $\sim 15\%$ of all β-decays. Shake off satellites may reach the detector directly following the magnetic field lines. To achieve a reasonable background rate in the mHz range demands an upper limit of $1-5$ mBq of T_2 for the main spectrometer volume, corresponding to a level of < 5 molecules per litre or a T_2 partial pressure of 10^{-19} mbar.

Trapped electrons will lead to an increase of the background rate as a function of final pressure of $\sim 10^{-9}$ Bq / mbar. This behavior has been observed in the spectrometers at Mainz and at Troitsk. To push the background rate down to a value of below 1 mBq, we have to minimize the number of trapped electrons by reducing their production rate and by significantly shortening their storage time. The latter task can be achieved by installing additional dipolar electrodes that can be switched on when no data are taken. As the time needed for emptying the spectrometer is in the ms range, this procedure can be repeated about every 10 s. Requiring a T_2 partial pressure in the mBq range and limiting the storage time of trapped electrons to 10 s means that the vacuum conditions in the spectrometer have to guarantee that *less than one single electron is trapped* in the spectrometer at any given time. At a pressure of 10^{-12} mbar one trapped electron would correspond to an increase of the background rate of 1 mBq [44)].

The XUHV pumping system of the KATRIN pre- and main spectrometer should therefore be designed to reach a final pressure of $p_{tot} < 10^{-11}$ mbar. Presently, the Mainz spectrometer is being modified with the aim to experimentally clarify the trapping and removal of electrons. Similar procedures and tests will be performed with the Troitsk spectrometer and especially with the KATRIN pre-spectrometer which acts as a test bed for all XUHV techniques applied to the main spectrometer. As a result of these experiments, the final demands on the XUHV conditions in the KATRIN main spectrometer can be specified in more detail.

3.5.3 XUHV methods

Currently we are investigating different methods to achieve an ultra high vacuum below 10^{-11} mbar in large recipients. In a first step the vacuum equipment of the existing Mainz spectrometer system has been upgraded and UHV conditions before and after the upgrade can be compared in the nearer future. Secondly, extensive UHV tests with the KATRIN pre-spectrometer will be performed later this year.

The 'reference' vacuum set-up for the initial pre-spectrometer vacuum tests will be based on cascaded turbomolecular pumps (Ebara TMPs) with a high compression ratio as well as on SAES getter strips (see also sect. 3.4). This set-up should efficiently block H_2 backdiffusion. In addition, the KATRIN pre-spectrometer vessel will be equipped with an oil-based heating/cooling system, that will allow to bake out the vessel at $350\,^{\circ}$C and to operate the spectrometer at $-20\,^{\circ}$C. At this operating temperature, the outgassing rate of hydrogen from the inner pre-spectrometer surfaces is suppressed by about one order of magnitude compared to room temperature.

An alternative vacuum concept for the KATRIN pre-spectrometer would be to separate it into two subsystems, with one subsystem used for conditioning, while the other would be used for maintaining the XUHV conditions. The conditioning system would consist of two TMPs in series which are equipped with forepumps. This subsystem would be mechanically isolated by a gate valve and could be turned off once XUHV conditions have been reached. The system for maintaining XUHV conditions would then consist of a getter pump and a sputter ion pump.

In both configurations, the getter material is housed in an external port (see fig. 15).

In a Monte Carlo based optimization procedure two geometrical patterns for the SAES getter strips were considered. For sticking coefficients of H_2 molecules on SAES getter material of 1 % the MC calculations yielded a pumping probability between 20 % and 30 %. A third geometrical model for the getter strips is currently being investigated with the aim to combine mechanical and vacuum technical aspects into an optimized solution.

The two vacuum concepts discussed above do not rely on coating processes of the inner surfaces of the KATRIN pre-spectrometer. As a further alternative, we are currently investigating the possibility of using a metallic coating on the wall interiors to reduce the hydrogen load on the getter pump. Several promising technologies are under investigation.

In this regard, an interesting new getter pumping method has recently been described in [52]. This concept is based on thin films of TiZrV getter material, which are sputter-deposited onto the inner vessel walls. The pumping by non-evaporable thin getter films would be supported by external TMPs. This new concept has been developed in the framework of the LHC project at CERN and would directly reduce the hydrogen outgassing rate. However, there are open questions and problems related to the concept of internal coating with sputter-deposited getters. The most important one is the possible migration of very small trace amounts of T_2 molecules to the spectrometer system. In this case, T_2 molecules would be pumped by the surface getter material. This would result in an increase of the background rate due to the β-decays of the pumped tritium. As the cleaning of the spectrometer vessel with sputter-deposited getter material at the inner surfaces would be a technological challenge, this approach is considered as backup solution at the moment. Further investigations of this technique will be performed in the nearer future with a vacuum test chamber at FZK (see sect. 3.4.1).

3.6 Magnet system

The magnet system of KATRIN has been further investigated with respect to design, operation, operational safety questions and economic optimization. This process has had its first outcome in the definition and tender action for the two pre-spectrometer magnets, which will be used in the first electromagnetic pre-spectrometer measurements in 2003 (see sect. 3.4). The magnet parameters are: central field 4.5 T, winding inner diameter 48 cm, warm bore 40 cm, length of winding pack 32 cm, operating current 200 - 500 A. The magnets will be equipped with a superconducting persistent current switch which guarantees that the magnetic field change will be significantly smaller than the required 2 % over a period of 3 months. While the two pre-spectrometer magnets have only negligible force action onto each other due the large distance of 430 cm, the neighbouring transport magnets lead to asymmetric forces on the pre-spectrometer magnets in the order of tens of tons.

A difficult tender demand for the magnet manufacturers is the requirement of the magnets to be fail-safe in case of quench at the maximum attainable (short sample) current in the persistent mode operation. This requirement has been set by us because quench tests will be performed that take the magnets beyond the operating current in order to get information about the operational safety margin. The pressure rise within the helium vessel due to the energy dump during the quench of a magnet can safely be handled and the German TÜV regulations for pressure vessels at low temperatures can be fulfilled.

With respect to cryogenic questions of the magnet system, various cooling concepts have been investigated under technological and economical view. The requirement of a safely continued operation of 4 days under the condition of a lack of coolant supply favours the use of liquid helium cooling but a cryocooler concept for at least a part of the magnet system is still under consideration for the case that the manufacturers' offers for such a system turn out to be more economic. If all magnets and the cryotraps are cooled with liquid helium, a rough estimate of the required cooling power leads to a refrigerator of about 300 W cold power. More detailed studies are under way, but all magnet positions and all heat loads have to be fixed before the final calculations of the cooling system will be performed.

3.7 Detector

Electrons with energies close to the tritium β-decay endpoint at 18.6 keV are transmitted through the KATRIN electrostatic filter system and are guided by two transport solenoids to the detector for counting purposes. The detector is required to have a good energy resolution, a good time resolution (for the ToF-mode) as well as a high electron efficiency together with a low sensitivity for environmental background gammas and X-rays. At the same time the detector should have a small backscatter probability for 20 keV electrons, a good position resolution to map the source profile. Finally, the detector should have the ability to operate for long periods of time in an XUHV environment and in strong magnetic fields. A comprehensive list of the specific requirements for the detector is given in table 1.

There are two principle detector options under consideration: a) semiconductor (sc) based detectors as well as b) thermal microcalorimeters (bolometers). The two types of detectors can be characterized as follows: semiconductor based detectors offer a rather good energy resolution (below 600 eV for 20 keV electrons, the resolution depends on the actual type of detector) and offer a time resolution of better than 1 μs, which would allow to perform standard tritium measurements as well as differential measurements of the T_2 spectrum in the MAC-E-TOF mode. On the other hand, microcalorimeters would allow to measure the β-electron energy with a resolution of 20-50 eV, which is one order of magnitude better than the resolution of sc based detectors.

There are challenges common to both detector types, especially with regard to implementing a segmented large area detector with minimized insensitive areas. Also, background from γ's from environmental activity and β-electron induced reactions have to be avoided. The latter tasks require an optimized passive shielding as well as careful selection processes for high-purity low-level materials in the proximity of the detector.

In the following we discuss several sc based detector options as well as the bolometer read-out option in more detail and report on the actual status of on-going tests

Requirement	Standard value	Parameter range	Remark
Electron energies E	18.6 keV	10 - 100 keV	
Sensitive area	$8.3 \times 10^3\,\mathrm{mm}^2$	$(7.5-10) \times 10^3\,\mathrm{mm}^2$	circular area
Energy resolution $\Delta E_{Det.}$ (FWHM at E=18.6 keV)	< 600 eV	250 - 600 eV 20 - 50 eV	for sc-based detectors for bolometers
Position resolution $(\delta x \cdot \delta y)$	$5 \cdot 5\,\mathrm{mm}^2$	$\delta x, \delta y < 5$ mm	source profile mapping
Time resolution	$\delta t = 0.1\,\mu s$	$\delta t = 0.1 - 1\,\mu s$	TOF-mode, calibration
Detector bulk material	Si Si, Be, other low Z		sc-based detectors bolometers
Detector thickness	$d = 300\,\mu m$	$d = 10 - 300\,\mu m$	$300\mu m$ is industrial standard, in general, as thin as possible
Dead layer entrance window	$\lambda < 50\,nm(Si)$ no dead layer	$30\,nm < \lambda < 50\,nm(Si)$	for p-doped entrance windows for bolometers
Insensitive areas	$\varepsilon < 5\%$	$\varepsilon < 10\%$	
Operation in magnetic fields	3 T	2.5-4 T	
background rate at 18.6 keV	$< 10^{-3}$counts/keV/s $< 10^{-2}$counts/keV/s	- -	sc based detectors bolometers
Operating temperature T	170 K 10 mK	70 - 250 K < 100 mK	sc-based detectors bolometers
Passive shielding	low level lead/copper	thickness 1-2 cm	
ENC of electronics	< 22 e^-(rms)	< 68 e^-(rms)	22e^- => Fano noise = electr. noise 68e^- $\simeq 600eV(FWHM)$

Table 1: Summary of detector requirements.

of sc based detectors.

3.7.1 PIN-Diode arrays

An economic solution for counting β-electrons on a large area in the energy range of few tens of keV is the use of silicon pixel-detectors with single pixel sizes in the range of up to $5 \times 5\,\mathrm{mm}^2$. This detector type (sometimes called Si-pad detector) is produced in different geometries and sizes by several industrial manufacturers¶. As a recent example we mention a monolithic 12×10 array of $5 \times 5\,\mathrm{mm}^2$ pixels manufactured by Hamamatsu for the X-ray satellite mission MEGA[53)]. This detector has achieved an energy resolution of 2 keV for low energy $\gamma's$, i.e. the energy response is dominated by electronic noise. This performance can be improved with the use of cooling and a sophisticated low noise read-out with the first FET being placed near the pixel. Therefore an energy resolution of the order of 600 eV seems feasible with pixel detectors and arrays of single PIN-diodes. However, this resolution limit cannot be improved significantly, as the energy resolution of this detector type is dominated by the terminal capacity of several pF.

In the recent years two new types of sc-based detectors have been developed which push the energy resolution of these detectors close to the physical boundary defined by the Fano noise ($\Delta E \geq 220$ eV).

3.7.2 Monolithic SDD arrays

Silicon drift diodes (SDDs)[54)] are high resolution room temperature detectors which are used in X-ray spectroscopy [55)] and as tracking devices in high energy physics[56)]. This detector type achieves a good performance even at very high count rates. The SDD consists of a volume of fully depleted silicon in which an electric field with a strong component parallel to the surfaces drives the signal electrons towards a small size collecting anode with an extremely small anode capacitance. For the counting of β-electrons one has to select SDD-types with entrance windows on uniform electrical potential to avoid position dependent detection efficiencies. For commercially available single SDD's an energy resolution of the order of 150 eV (FWHM) or better has been achieved at the Mn Kα energy of E=5.9 keV. This is already close to the Fano noise for a 5.9 keV energy deposit in silicon which corresponds to 120 eV.

The instrumentation of the entire KATRIN flux tube with an area of $\sim 10^4$ mm^2 requires the implementation of a monolithic multi-element SDD array. With individual SDD areas of $5{\times}5$ mm^2 this would correspond to an array 400 single SDD elements. Up to now, the largest monolithic array in routine operation consists of 7 SDDs with single sensitive areas of 5mm^2 [57)]. Presently, a monolithic 61-element SDD array is under development in an European project [58)]. The construction of a significantly larger monolithic SDD array with several hundred elements would require a substantial R&D effort. The option of a monolithic SDD-array will be further

¶Hamamatsu, Eurisys-Canberra, Micron

investigated by a feasibility study in close collaboration with an industrial partner. First tests at FZK with a single SDD element are reported below.

3.7.3 DEPFET pixel matrices

The DEpleted P-channel Field Effect Transistor (DEPFET) [59] is a low noise pixel detector developed at the MPI Halbleiterlabor München with the first stage amplifier integrated into the detector. Typical pixel sizes are of the order of $50 - 150\,\mu$m. At the University of Bonn a 64×64 pixel matrix has been developed [60], which operates as Bioscope-System used for biomedical applications using samples with tritium markers. Measurements with a DEPFET pixel show a very good intrinsic energy resolution of 158 eV (FWHM) at $E_\gamma = 6$ keV [60], equivalent to an electronic noise contribution of ENC $= (12 \pm 1)\,\mathrm{e}^-$. The DEPFET principle allows to build novel pixel detectors with large areas for applications in high energy physics experiments and X-ray astronomy [61,62]. Due to the small capacity of each pixel these devices could also be produced much thinner than the current standard value of $300\,\mu m$. One of the challenges of this technology, if applied and scaled to the β-counting requirements of KATRIN, would be the read-out scheme for the $\sim 10^4$ channels per cm^2.

3.7.4 Bolometers

Thermal microcalorimeters (bolometers) offer the possibility to achieve a superior energy resolution of about 20-30 eV for β-electrons in the energy range above a few keV. This type of detector is in use for neutrinoless double beta decay searches [63] (Mi-Beta [64], Cuoricino [32], Cuore [33]), dark matter (WIMP) searches and β-decay spectroscopy to measure the electron neutrino mass (Munu2 [65]).

The absorber material of the bolometers can be a low-Z material which minimizes background from environmental gammas. A feasible absorber material would be Be.

There are two types of semiconductor based thermistors which can be used as sensors for the read-out of microcalorimeters in strong magnetic fields of several Tesla: a) silicon implanted and b) NTD germanium thermistors. Silicon implanted thermistors have been developed in the in framework of $0\nu\beta\beta$ searches[69]. Their major advantages are the reproducibility and the possibility of large scale productions. Work is in progress to implement micromachining techniques to build fully integrated thermistors. For KATRIN, a thin Si-implanted thermistor would have to be used, with the absorber dominating the heat capacity. The second type of thermistors, so-called NTD-germanium thermistors will be used for the $0\nu\beta\beta$-experiments Cuoricino and CUORE. Their production process is however rather sophisticated. The characteristics of this thermistor type are described in more detail in [66].

The implementation of a bolometer array would be technologically challenging, given the requirements of microcalorimeters with regard to their operating temperatures in the mK range. A dilution refrigerator with horizontal cold finger would provide the required operational temperature, however, the 'open' geometry required for the counting of the β-electrons would be challenging, taking into account the incoming radiation flux from the main spectrometer which is operated at a temperature of 250 K. A suppression of this heat load to the bolometer would require at least two additional transport elements with LHe bore. Nevertheless, a bolometric read-out for KATRIN seems to be feasible. In particular, one could make ideal use of existing thermistor techniques, which have been developed for double beta decay searches [33], as well as of recently reported improvements with regard to noise suppression [67] and read-out stabilization [68].

3.7.5 Status and Outlook

Presently we are investigating the properties of two commercially available SDD detectors (KETEK and Canberra) using the X-ray fluorescence beam line of the ANKA synchrotron radiation source at FZK as well as X-ray fluorescence sources in the mCi range [70]. First tests show promising results and verify that this type of detector will allow to achieve an energy resolution close to the Fano noise limit. Further tests with an electron gun from Troitsk will be performed later this year with the aim to investigate in detail the detector performance for electrons in the keV range. The results of these tests with regard to energy resolution, energy losses in the dead layer and backscatter probability will be compared to corresponding simulations based on the GEANT4 low-energy simulation package [71]. In parallel, Si-pixel detectors will be investigated by XRF-techniques.

The characteristics of semiconductor based detectors and bolometers are summarized in table 2. The final choice between these two principle detector options will depend on the background rejection factors that can be expected. The superior energy resolution of a microcalorimeter array would only be useful if the background events are distributed either flat in energy around the retarding potential or if they would show a micro-structure on the few-tens of eV scale. In both cases a microcalorimeter would allow to strongly suppress background events. On the other hand, if the background events would be clustered very close to the retarding potential (with an energy spread of the order of a few eV) no improvement would be expected. This type of 'full energy' background is expected from low-energy electrons in the spectrometer: in this case background electrons in the few-eV range start close to the analyzing plane of the KATRIN main spectrometer and are re-accelerated and focused onto the detector where they appear clustered close to E_0. The structure of the background energy distribution is currently being investigated in the Mainz and Troitsk data. The aim of these on-going investigations is to provide experimental input for a decision among the two principle detector options for KATRIN.

3.8 Calibration and long-term monitoring

The high precision spectroscopy of β-electrons close to the endpoint of tritium at 18.6 keV requires a precise absolute calibration of the KATRIN electrostatic spectrometer.

	PIN-Diode-array Pad-Detector	SDD	DEPFETS	Bolometers
γ-energy resolution at E_γ = 6 keV	$\sim$ 300 eV (estimated)	175 eV (measured)	158 eV (measured)	20-50 eV (estimated)
position resolution	1-5 mm	1-5 mm	50 μm	1-5 mm
time resolution	0.1 μs	0.1 μs	20 μs	100 μs
dead layer	30-50 nm	30-50 nm	30-50 nm	window less
operating temperature	$-100°$	$-20°$	room temp.	10-100 mK

Table 2: Comparison of resolution figures and characteristics of different detector concepts.

Moreover, as the tritium measurements will take several years to accumulate the statistics for a sub-eV sensitivity, the long-term stability of the spectrometer system has to be monitored continuously. In the following we describe methods based on the K-32 conversion electron line of ^{83}Kr to calibrate and monitor the long-term stability of the KATRIN electrostatic spectrometer.

3.8.1 Calibration with K-32 conversion electrons from gaseous ^{83m}Kr

The K-32 conversion electron line from gaseous ^{83}Kr has an energy of 17.8 keV. As this energy differs by only 0.8 keV from the endpoint energy of the tritium β-spectrum, the K-32 line is well suited for the tasks of the absolute calibration and the monitoring of the spectrometer energy scale. For the first task, the energy of this conversion line has to be known with high precision. A previous measurement [72] of the K-32 conversion electron energy of $(17\,821.4 \pm 2.0)$ eV is not sufficiently accurate for the KATRIN experiment. In the following we outline an experimental programme to improve the precision of this value.

For ^{83}Kr atoms in gaseous form, the electron kinetic energy E_{kin} of the K-32 conversion line measured by an electrostatic spectrometer is given by

$$E_{kin} = E_\gamma + E_{\gamma,rec} - E_b\,(\text{vac}) - E_{e,rec} - (\phi_{spectr} - \phi_{source}) \tag{12}$$

Here, E_γ is the γ-ray energy, E_b (vac) is the binding energy of K-shell electrons related to the vacuum level, $E_{\gamma,rec}$ = 0.0067 eV is the energy of the recoil atom after γ-ray emission and $E_{e,rec}$ = 0.120 eV is energy of the recoil atom after conversion electron emission. The parameters ϕ_{spectr} and ϕ_{source} are the work functions of the spectrometer and the Kr-source vacuum chamber, respectively.

The experimental precision for the above parameters is the following: the γ-ray energy E_γ has been determined by semiconductor detectors [73,74] with an uncertainty of $\pm$ 1.6 V relative to the ^{241}Am standard of [75]. We have recalibrated the results obtained in [73,74] according to the new ^{241}Am standard of [76] and calculated a new weighted average of $E_\gamma = (32\,151.55 \pm 0.64)$ eV. We plan additional measurements of the γ-ray energy E_γ using HPGe and Si(Li) detectors with improved energy resolutions of ΔE = 230 and 290 eV (FWHM) at 32 keV, respectively.

Two different methods were employed for the determination of the binding energy of K-shell electrons $E_b\,(\text{vac})$: a) the photoabsorption of monochromatized synchrotron radiation [77], yielding $E_b\,(\text{vac}) = (\,14\,327.2 \pm 0.8\,)$ eV, and b) a combination of X-ray diffraction studies with X-ray excited photoelectron spectroscopy (XPS) on higher atomic shells. In [78] four alternative transition combinations of $K\,\alpha_1$, $K\,\alpha_2$, $K\,\beta_1$ and $K\,\beta_2$ wavelengths with corresponding electron binding energies [80] were utilized. These measurements delivered a value of $E_b\,(\text{vac}) = (\,14\,327.1 \pm 0.45\,)$ eV. The weighted average of the two different methods is $E_b\,(\text{vac}) = (\,14\,327.09 \pm 0.39\,)$ eV.

Inserting the above values into eq. (12) one derives a value for the electron kinetic energy of

$$E_{kin} = [\ (\,17\,824.35 \pm 0.75\,) - (\,\phi_{spectr} - \phi_{source}\,)\ ]\ \text{eV}.$$

A precise method to determine the difference in work functions (ϕ_{spectr} - ϕ_{source}) of the KATRIN main spectrometer and the WGTS would be the use of bunches of low energy monoenergetic electrons of about 35 eV energy and natural widths in the meV range which result from doubly excited ^{4}He auto-ionization states (this technique is described in more detail in sec. 3.2.4). Alternatively, we are considering to use the LMM Auger electrons of krypton with an energy of about 1.5 keV.

3.8.2 Long-term monitoring with K-32 conversion electrons

To achieve a neutrino mass sensitivity of 0.35 eV with the KATRIN main spectrometer, the actual value of the retarding potential in the 18.6 kV range has to be known to a precision of a few ppm. This requires the long-term monitoring of the retarding voltage over the entire KATRIN measurement time of several years. Therefore it is highly desirable to rely not only on high quality electrical measurements[‖] but to employ also a physical *reference* based on a stable monoenergetic electron source.

We thus consider long-term monitoring of the high voltage of the KATRIN main spectrometer by means of a separate K-32 conversion electron source. This source would be used exclusively for monitoring purposes and would have to be connected to a third electrostatic spectrometer ('monitor spectrometer'). In this regard, a conceivable and economic solution would be to make use of the existing Mainz spectrometer, which would have to be transferred to FZK and to be installed at the KATRIN experimental hall. The close proximity of the KATRIN main spectrometer and the monitor spectrometer would allow to feed both filters by a common high voltage. As the tritium end-point lies at 18.6 keV and the monitor Kr-source provides energies of 17.8 kV, the conversion electrons would have to be accelerated to the tritium endpoint region *before* being analyzed in the middle plane of the monitoring spectrometer. The precise measurement of this accelerating voltage does not represent a technical problem as it would be below 1 kV.

[‖] It seems feasible to construct a HV divider which is constant within 2 ppm in the $\pm$ 10 % interval around the nominal voltage [83].

This type of monitoring source could technically be realized in the form of a thin ^{83}Kr film condensed onto a cold backing that was extensively studied in [79]. For this configuration of a quench condensed monitor source (QCMS) one could additionally rely on a theoretical correction of (-2.4 ± 0.2) eV to E_b (vac) in eq. (12). The electron spectroscopy value of $E_\gamma = (32\,151.5 \pm 1.1)$ eV involving this correction is in excellent agreement with the γ-spectroscopic average of $E_\gamma = (32\,151.55 \pm 0.64)$ eV.

Since the half-life of ^{83m}Kr is 1.8 hours only, a repeated condensation would be necessary. Cleaning of the backing surface with a laser beam and application of a new pure ^{83m}Kr gas batch for condensing onto the cold substrate should guarantee the reproducibility of the conditions and thus the stability of the conversion electron energy E_{kin}. Another possibility would be to attempt the continuous condensation of ^{83m}Kr with appropriate desorption of ^{83}Kr to avoid the source charging.

We are currently examining the possibility to employ a vacuum evaporated thin layer of ^{83}Rb (half-life of 86 days) as a continuous source of ^{83m}Kr in situ. In [81] this approach was applied to investigate Auger electron spectra of krypton. Further investigations will have to clarify the following open questions: a) will the ^{83}Rb compounds escape from the backing at ultrahigh vacuum conditions of $\simeq 10^{-9}$ mbar and penetrate to the spectrometer and b) will the K-shell binding energy change during successive transformations of rubidium into krypton.

Presently, a vacuum chamber equipped with a quadrupole mass spectrometer is under construction to inspect the behavior of rubidium compounds at UHV conditions. At the same time, a very high resolution electrostatic electron spectrometer at JINR in Dubna (Russia) is modernized to examine the time stability of the K-32 line energy with the help of a composite ^{83}Rb + ^{57}Co + ^{169}Yb source prepared by vacuum evaporation. A new computer control of the electrostatic spectrometer at NPI/Rez near Prague (Czech Republic) is being developed to allow long-term measurement of true secondary electrons emitted from the ^{83}Rb source with eV energies. This would allow to recognize possible changes of the source surface.

3.8.3 Consistency tests and simulations

The experimental investigations with regard to the tasks of calibration and monitoring are complemented by extensive Monte-Carlo simulations of tritium β-spectra. These studies have the impetus to investigate on a quantitative level the influence of uncertainties in the energy calibration and imperfections in the long-term HV stability on the deduced neutrino mass. In addition, we have performed model independent statistical tests of the stability of the KATRIN measurement conditions. These studies are based on earlier work [82] and have been extended to simulated β-spectra which correspond to the expected signal spectra in the KATRIN integral spectrometer. This technique allows to reveal discrepancies among partial β-spectra corresponding to slightly different conditions with great sensitivity. An alternative approach to investigate the consistency of the KATRIN data set would be to fit the end-point energy in partial β-spectra and to examine the consistency of the fitted values. This method has already been successfully applied in tritium measurements at NRI in Troitsk (Russia).

3.9 Project Schedule and Costs

Following the publication of the KATRIN Letter of Intent [1)], the collaborating universities of Karlsruhe and Mainz successfully applied for support from the German BMBF 'Astroparticle' fund. This funding is initially for a 3 year period covering the calendar years 2001-04. These funds are of the order of 10 % of the total project hardware costs and will be used for the design, the construction and the commissioning of the KATRIN pre-spectrometer. In addition, the funds will allow to contribute to the running costs of the pre-spectrometer and to upgrade the Mainz set-up to perform detailed background studies with the Mainz spectrometer.

Work on the construction of the pre-spectrometer has started already in 2001 with the ordering of a stainless steel batch for the pre-spectrometer and extensive vacuum equipment (TMPs, vacuum gauges etc.). In the first half of 2002, the pre-spectrometer will be commissioned, and the second half of 2002 will be dedicated to extensive vacuum tests with the pre-spectrometer set-up. In parallel, the first two superconducting magnets for pre-spectrometer are about to be ordered (the tender action is still on-going). With an estimated production time of 9-12 months this schedule will allow to test the electromagnetic properties of the pre-spectrometer in early 2003 (by this time the inner electrode system as well as an electron gun will be available). By the end of 2003 detailed investigations of the electromagnetic properties of the pre-spectrometer will have been performed. This knowledge, as well as earlier expertise with regard to vacuum issues, will be of crucial importance for the further design of the main spectrometer.

On condition that the funding requests to German (Hermann von Helmholtz-Gemeinschaft Deutscher Forschungszentren [HGF], in particular the astroparticle physics funding within the HGF 'structure of matter' programme) and international funding agencies will be successful, the KATRIN experiment could be built up by 2006, so that first test measurements could start some time later in 2007. This time frame is based on a detailed project schedule for KATRIN, which has been further refined since the publication of the LoI. The total measurement time will be of the order of 5 years, requiring a continuation of resources for the running of KATRIN. This 5 year running schedule is based on the required measuring time of ~ 1000 days for normal tritium runs to reach the final sensitivity of 0.35 eV at 90 % CL.

The total project costs are estimated to be 22 M Euros, with the major costs arising from the system of more than 30 superconducting solenoids (7.8 M Euros), the spectrometers (4.5 M Euros), the tritium sources (2.6 M Euros), the cryosupply (2.8 M Euros) as well as other items (experimental hall, vacuum pumping, detector and common funds). It is expected that the majority of the required financial resources will be provided by funding from the HGF.

Finally it should be mentioned that the Collaboration is aiming at further strengthening the project by enlarging the Collaboration. Over the past months detailed discussions have been taken place with several groups which are interested in the physics and techniques of KATRIN. New potential collaborators have been identified, which would be willing to take over specific tasks within the KATRIN project schedule and which could bring in further expertise and resources.

4 References

1) A. Osipowicz et al. (KATRIN Collab.), `hep-ex/0109033`, FZKA report 6691
2) Y. Farzan, O.L.G. Peres, A. Yu. Smirnov, Nucl. Phys. **B612** (2001) 59
3) S.M. Bilenky, S. Pascoli, S.T. Petcov, Phys. Rev. **D64** (2001) 113003
4) A.D. Dolgov, `hep-ph/0202122`
5) X. Wang, M. Tegmark, M. Zaldarriaga, `astro-ph/0105091`
6) R.A.C. Croft, W. Hu, R. Davé, Phys. Rev. Lett. **83** (1999) 1092
7) M. Fukugita, G.-C. Liu, N. Sugiyama, Phys. Rev. Lett. **84** (2000) 1082
8) M. Tegmark et al., `astro-ph/0107418`
9) Ø. Elgarøy et al., `astro-ph/0204152`
10) M. Tegmark, M. Zaldarriaga, A.J.S. Hamilton, Phys. Rev. **D63** (2001) 043007
11) M. Tegmark, priv. communication (2002)
12) J.R. Primack, M.A.K. Gross, in D. O. Caldwell (ed.): Current Aspects of Neutrino Physics (Springer, Berlin Heidelberg, 2001)
13) A.D. Dolgov et al., `hep-ph/0201287`
14) P. Vogel, `nucl-th/0111016`
15) J.F. Beacom, R.N. Boyd, A. Mezzacappa, Phys. Rev. **D63** (2001) 073011
16) J.F. Beacom, R.N. Boyd, A. Mezzacappa, Phys. Rev. Lett. **85** (2000) 3568
17) N. Arnaud et al., Phys. Rev. **D65** (2002) 033010
18) T. Weiler, Phys. Rev. Lett. **49** (1982) 234
19) Z. Fodor, S.D. Katz, A. Ringwald, `hep-ph/0203198`
20) A. Ringwald, `hep-ph/0111112`
21) Z. Fodor, S.D. Katz, A. Ringwald, `hep-ph/0105064`
22) K.S. Capelle et al., Astropart. Phys. **8** (1998) 321
23) Q.R. Ahmad et al., Phys. Rev. Lett. **87** (2001) 071301
24) Q.R. Ahmad et al., `nucl-ex/0204008`
25) Q.R. Ahmad et al., `nucl-ex/0204009`
26) F. Feruglio, A. Strumia, F. Vissani, `hep-ex/0201291`
27) S.R. Elliott, P. Vogel, Annu. Rev. Nucl. Part. Sci. **52** (2002)
28) H.V. Klapdor-Kleingrothaus, *"60 Years of Double Beta Decay - From Nuclear Physics to Beyond the Standard Model"*, World Scientific, Singapore (2001)
29) H.V. Klapdor-Kleingrothaus et al., Eur. Phys. J. **A12** (2001) 147
30) H.V. Klapdor-Kleingrothaus et al., Mod. Phys. Lett. **A16** (2002) 2409
31) C.E. Aalseth et al., `hep-ex/0202018`
32) A. Alessandrello et al., Nucl. Phys. **B87** (2000) 78

33) A. Alessandrello et al., `hep-ex/0201038`
E. Fiorini, Phys. Rep. **307** (1998) 309
34) S. Pascoli, S.T. Petcov and L. Wolfenstein, Phys. Lett. **B524** (2002) 319
35) S. Pascoli, S.T. Petcov, `hep-ph/0111203`
36) M. Czakon, J. Gluza, J. Studnik, M. Zralek, Phys. Rev. **D65** (2002) 053008
37) S. Pascoli, S.T. Petcov, `hep-ph/0205022`
38) V.M. Lobashev, talk given at NANP01, Dubna, June 2001
39) J. Bonn *et al.*, Nucl. Phys. **B**(Proc. Suppl.) **91** (2001), 273
40) Ch. Kraus, talk at the DPG spring meeting, Münster, March 2002
41) V. Lobashev *et al.*, Nucl. Phys. **B**(Proc. Suppl.) **91** (2001), 280
42) investigations carried out by P. Leiderer, Univ. of Konstanz (Germany)
43) D.J. Taylor, M. Glugla, R.-D. Penzhorn, Rev. Sci. Instrum. **72** (2001) 1970.
44) J.-P. Schall, diploma thesis, Mainz university, 2001
45) H. Ulrich, diploma thesis, Mainz university, 1999
46) C. Kraus, PhD thesis, Mainz university, to be finished in 2002
47) T. Thümmler, diploma thesis, Mainz university, 2002
48) B. Müller, diploma thesis, Mainz university, to be finished in 2002
49) L. Fickinger, diploma thesis, Mainz university, 2000
50) B. Flatt, diploma thesis, Mainz university, 2001
51) B. Flatt, PhD thesis, Mainz university, in preparation
52) C. Benvenuti et al., Vacuum **60** (2001) 57
53) P. Weilhammer et al., Nucl. Instr. Meth. **A383** (1996) 89
54) E. Gatti, P. Rehak, Nucl. Instr. Meth. **A225** (1984) 608
55) P. Leutenegger et al., Nucl. Instr. Meth. **A439** (2000) 458
56) P. Holl et al., Nucl. Instr. Meth. **A377** (1996) 367
57) P. Kappen et al., Nucl. Instr. Meth. **A467** (2001) 1163
58) K. Hansen, Larc Tröger, IEEE Trans. on Nucl. Sci., Vol **47**, No. 6 (2000)
59) J. Kemmer, Nucl. Instr. Meth. **A253** (1987) 365
60) W. Neeser et al., Nucl. Instr. Meth. **A477** (2002) 129
61) G. Lutz et al., Nucl. Instr. Meth. **A461** (2001) 393
62) P. Holl et al., IEEE Trans. Nucl. Sci., Vol. **47**, No. 4 (2000)
63) O. Cremonesi, in Proc. of the 9th Int. Workshop on Low Temperature Detectors (LTD-9), Ed. F.S. Porter, AIP Conf. Proceed. Vol. **65** (2002) 443
64) S. Pirro et al., *ibid*, p. 449
65) F. Gatti, *ibid*, p. 429
66) J. Beeman et al., *ibid*, p. 211
67) S. Pirro et al., Nucl. Instr. Meth. **A444** (2000) 331
68) A. Alessandrello et al., Nucl. Instr. Meth. **A412** (1998) 454
69) A. Alessandrello et al., J. Phys. D: Appl. Phys. **32** (1999) 3099
70) T. Kepcija, diploma thesis in preparation, Karlsruhe university, 2002
71) F. Schwamm, PhD thesis, Karlsruhe university, in preparation
72) W. Stoeffl, D.J. Decman, Phys. Rev. Lett. **75** (1995) 3237
73) S.T. Staggs et al., Phys. Rev. **C39** (1989) 1503

74) V.M. Gorozhankin et al., Proc. 43^{rd} Ann. Conf. Nucl. Spectrosc. Struct. at Nuclei, Dubna, (1993) p. 181
75) G.C. Nelson, B.G. Saunders, Nucl. Instr. Meth. **84** (1970) 90
76) R.G. Helmer, C. van der Leun, Nucl. Instr. Meth. **A450** (2000) 35
77) M. Breinig et al., Phys. Rev. **A22** (1980) 520
78) R. D. Deslattes et al., Int. Tables for Crystallography, 2^{nd} Edition, Ed. A.J.C. Wilson and E. Prince, Kluwer Acad. Publishers, Norwell, Mass. (1999) p. 200
79) A. Pickard et al., Z. Phys. **A342** (1992) 71
80) K. Siegbahn et al., ESCA applied to Free Molecules, North Holland, Amsterdam, 1969
81) A. Kovalik et al., J. Electron Spectr. Relat. Phenom. **58** (1992) 49
82) O. Dragoun et al., Nucl. Instr. Meth. **A391** (1997) 345
83) R. Marx, IEEE Trans. Instr. Meas. Vol. 50, No. 2, 2001